(12)

MODIFICATION OF THE NEAR SURFACE REGION METASTABLE PHASES AND ION INDUCED REACTIONS

Final Technical Report

1 April 1980 to 30 September 1983

ONR Contract: N00014-80-C-0479
DARPA Order 3957

Submitted to

Office of Naval Research
(L. Cooper)

DARPA (S. Roosild)

Short Title: "Metastable Solid Phases"

Principal Investigator

James W. Mayer
(607) 256-7273

3 February, 1984

TABLE OF CONTENTS

"Metastable Solid Phases"

I. Objectives

The investigation was directed toward the formation and characterization of amorphous and crystalline metastable structures formed in the near-surface region of solids. The initial objective was to establish a backscattering and channeling facility.

II. Accomplishments

A. Rutherford Backscattering Facility

The accelerator (Tandetron Analyzer System with 1.0 MV terminal voltage) was delivered 6 July, 1981 (original delivery date was 1 Nov. 1980). General Ionex installation personnel arrived 13 July, 1981. The first backscattering spectra at 2.4 MeV He^{++} were obtained 24 July, 1981 - and spectra at the oxygen resonance at 3.04 MeV He^{++} obtained on 31 July, 1981. There were a number of adjustments and modifications to the beam line and chamber required before the system was ready for routine operation. In 1982, the Rutherford Backscattering Facility was in use by the research group engaged in studies of metastable solid phases. In 1983, the facility was in routine use and was made available to other research groups.

The availability of a Rutherford Backscattering Facility has made a significant impact on the Cornell research community that deals with electronic materials, thin film structures, molecular beam epitaxy and ion implantation.

The impact is due to the growth in the number of Cornell users of the Rutherford Backscattering Facility. In the past year, accelerator users have included over 60 graduate students and faculty from Materials Science, Electrical Engineering, Physics, Applied Physics, Chemistry, Chemical Engineering and Anthropology. Appendix A lists graduate students in the Thin Film Interactions

group of Prof. Mayer who carry out research with backscattering and channeling measurements. Appendix B lists the visiting scientist and research associates working with group. Appendix C lists the Cornell and Appendix D lists the outside of Cornell users of the facility.

Cornell has a tradition of interdisciplinary research but this appears to be the first time that one analytical instrument has brought about such campus-wide interest. The attractive feature of backscattering analysis is that it provides a direct measurement, easily visualized from the data, of composition depth profiles. Furthermore, sample analysis can be carried out in 15 to 20 minutes by a user with only a few hours of instruction. For groups dealing with thin-film deposition and reactions, epitaxial growth and semiconductor contact metallization it is imperative to have ready access to such a quantitative analytical instrument.

Aside from routine measurements, there have been a number of important new developments. In one case Professor Kramer found that he could exploit the depth resolution in backscattering to obtain a near-four order of magnitude improvement in the analysis of interdiffusion in organic films. This is a new application which opens up an exciting field of study. In another case we have found that composition analysis can be carried out directly on 500 to 1000 Å thick films mo[illegible]d on transmission electron microscope grids. This allows a direct comparison of composition and structure. By the use of a detector mounted for forward scattering, we have been able to measure hydrogen profiles in hydrogenated amorphous-silicon. Using the combination of ion-induced X-rays and backscattering, the anthropologists are actively investigating the evolution of pottery glazing techniques.

We continue to develop the analytical capabilities to add, for example, detection systems for gamma rays for nuclear reaction depth profiling of Al in

in GaAlAs/GaAs heterojunction structures. We are developing the analysis of 100 micron diameter optical fibers to determine coating thicknesses. We continue to improve our computer-based programs for data analysis.

B. Melt-Front Kinetics

The dynamics of silicon solidification from the melt during pulsed-ruby-laser annealing of bulk Si crystals and Si on sapphire have been investigated with the use of time-resolved electrical-conductance and optical reflectance. Bulk Si samples were used to determine the resolidification velocities and to compare the experimental results with numerical calculations based on a thermal model for laser melting. Si on sapphire samples were used because the photo-conductive contribution to the transient current was sufficiently small so that the entire melt and resolidification process could be directly observed. The transient conductance technique yields quantitative measures of melt depths, melt-in velocities (5 to 13 m/s) and solidification velocities (2.8 to 3.3 m/s).

The importance of the transient conductance technique (developed in 1981-1982 under DARPA/ONR sponsorship) is that it provided for the first time a direct measure of melt depths during laser annealing. The availability of an in-situ measurement of melt dynamics allowed us to cut through much of the mystery and controversy surrounding laser annealing and to place the field on solid footing.

The details of the measurements are described in publications (No. 2, 6 and 8 of Section IV of this report) and comments on pulsed laser irradiation of silicon and the development of the transient conductance technique are given in Section V. 1.

C. Amorphous and Crystalline Phase Formation

The effect of ion beam mixing on multilayer samples in the Al/Pt, Al/Pd and Al/Ni systems has been studied with TEM techniques. The phases PdAl and NiAl are the only equilibrium alloys found in ion beam mixing, while the

amorphous phase has been observed over a large range of compositions. We believe that the different behavior is related to the difference in the crystalline structure of the equilibrium compounds. With ion irradiation, crystalline phases of simple structures, such as solid-solutions or simple cubics, can be formed while amorphous structures are formed with more complex structures.

With ion-mixing of bilayers of Ni containing 1.5 atomic % Au, we found that ion mixing formed silicides but the Au segregated to the Ni/Ni-silicide interface. The same behavior, that is the segregation of Au at the interfaces, has been found in thermal annealing. This implies that thermodynamic driving forces are dominant in ion beam mixing. If recoil collisions and ballistic effects dominated, the Au atoms would not show a sharp concentration profile at interfaces.

The details of the measurements are described in publications (Nos. 1, 3, 7, 9 and 10 in Section IV). A longer description of phase formation in metal-metal systems is given in Section V.

D. NATO Advanced Research Institute on "Surface Modification by Directed Energy Processing"

The contract was supplemented in 1981 by $9,600 to provide travel support for 9 U.S. scientists to participate in a NATO Institute whose subject was directly in line with the thrust of this contract. The group met in Trevi on 24-28 August 1981 and at Cornell 10-13 January, 1982. The publication of the proceedings is "Surface Modification and Alloying", edited by J.M. Poate, G. Foti and D.C. Jacobsen, Plenum Press, 1983.

III. Scientific Personnel and Ph.D. Theses

A. Ph.D. Theses of Students Whose Research Was Supported in Part by the DARPA/ONR Program

1. Liquid Solid Interface Dynamics During Pulsed Laser Melting of Silicon on Sapphire.

   Michael O. Thompson, Jan. 1984

2. Ion-Beam-Mixing in Metal-Metal Systems and Metal-Silicon Systems.

   Liang-Sun Hung, Jan. 1984

B. Cornell Personnel Whose Research Was Supported in Part by the DARPA/ONR Program

James W. Mayer

Lih J. Chen (Visiting Scientist, Tsing Hua University)

Jozsef Gyulai (Central Research Institute of Physics)

Chris J. Palmstrom (Postdoctoral Fellow)

Larry S. Doolittle

Richard Fastow

Greg J. Galvin

Liang-Sun Hung

Michael Nastasi

Michael O. Thompson

Long-ru Zheng

C. Investigators at Other Laboratories Who Were Involved in Collaborative Research on the Cornell DARPA/ONR Program

Paul S. Peercy - Sandia National Laboratories

Robert B. Hammond - Los Alamos National Laboratories

IV. Publications acknowledging work supported in part by DARPA (S. Roosild) through ONR (L. Cooper)

1) Transmission electron microscope study of ion beam induced interfacial reactions in molybdenum thin films on silicon

L.J. Chen, L.S. Hung, J.W. Mayer

Applications of Surface Science 11, 202-208 (1982)
June 1981

2) Measurement of the velocity of the crystal-liquid interface in pulsed laser annealing of Si

G.J. Galvin, M.O. Thompson, J.W. Mayer
R.B. Hammond, N. Paulter (Los Alamos National Laboratories)
P.S. Peercy (Sandia National Laboratories)

Phys. Rev. Lett. 48, 33-36 (1982)
October 1981
DARPA/ONR and DOE (Sandia)

3) Pulsed beams and ion-beam mixing: Metal-Si and metal-metal structures

F.X. Bonejumper, R. Fastow, G. Galvin, L.S. Hung, J.W. Mayer, M. Nastasi, M.O. Thompson, L.R. Zheng

Metastable Materials Formation By Ion Implantation, S.T. Picraux and W.J. Choyke, eds., (North Holland, New York, 1982), pp. 125-132
November 1981

4) (AlxGa1-x)0.47In0.53As: Growth and characterization

C.R. Stanley, D. Welch, G.W. Wicks, C.E.C. Wood
(School of Electrical Engineering)
C. Palmstrom
F.H. Pollack, P. Parayanthal (Dept. Physics, Brooklyn College)

Inst. Phys. Conf. Ser. No. 65, (The Institute of Physics, 1983), Chapter 3, Proceedings of the Int. Symp. on Gallium Arsenide and Related Compounds, Albuquerque 1982, pp. 173-180
June 1982

5) Electron Inelastic Mean Free Path (imfp) in single crystal BeO by Rutherford Backscattering (RBS) and Auger Electron Spectroscopy (AES)

D.E. Fowler, J. Gyulai, C. Palmstrom

J. Vac. Sci. Technol. A, 1, 1021-1025 (1983)
August 1982
DARPA/ONR and DOE and MSC (D.E.F.)

6) Time-resolved conductance and reflectance measurements of silicon during pulsed-laser annealing

G.J. Galvin, Michael O. Thompson, J.W. Mayer
P.S. Peercy (Sandia National Laboratories)
R.B. Hammond, N. Paulter (Los Alamos National Laboratories)

Phys. Rev. B27, 1079-1087 (1983)
September 1982
DARPA/ONR and DOE (Sandia)

7) Pulsed ion beam interface melting of PtCr and CrTa alloys on Si structures

C.J. Palmstrom, R. Fastow

Laser-Solid Interactions and Transient Thermal Processing of Materials, J. Narayan, W.L. Brown, R.A. Lemons, eds. (North Holland, New York, 1983), pp. 715-720
September 1982

8) Melt dynamics of silicon-on-sapphire during pulsed laser annealing

Michael O. Thompson, G.J. Galvin, J.W. Mayer
P.S. Peercy (Sandia National Laboratories)
R.B. Hammond (Los Alamos National Laboratory)

Appl. Phys. Lett. 42, 445-447 (1983)
September 1982
DARPA/ONR and DOE (Sandia)

9) Ion-induced amorphous and crystalline phase formation in Al/Ni, Al/Pd and Al/Pt thin films

L.S. Hung, M. Nastasi, J. Gyulai, J.W. Mayer

Appl. Phys. Lett. 42, 672-674 (1983)
January 1983

10) Thermal and ion induced reaction of Ni-Au dilute alloys on Si

L.S. Hung, L.R. Zheng, J.W. Mayer

J. Appl. Phys. (accepted for publication)
April 1983

V. Melt-Front Kinetics and Ion Beam Mixing

A. Laser Irradiation and Transient Conduction

(prepared by M.O. Thompson)

In 1977, Soviet workers first observed the ability of short pulse (less than ~50 ns) ruby and neodymium laser radiation to anneal the lattice damage associated with ion implanted surface layers [1]. This ability, and recently the ability to form new phases, has been intensely studied during the past 6 years [2-3]. The field has expanded since those early experiments to encompass not only technically important semiconductor processing possibilities, but also the more important fundamental mechanisms involved in ultra-fast melt and resolidification of materials. The field continues to expand today into topics as diverse as laser assisted sputtering [4] and metastable alloy formation [5].

In a sense, the laser has been used as little more than an extremely fast heat gun for the majority of this laser annealing work. Indeed, many of the original applications suggested for scanned continuous wave lasers have been implemented with conventional, and more economical, heat sources such as quartz-halogen lamps [6], graphite strip heaters [7] and electron beam sources [8]. However, the flexibility of the laser allowed development and experimentation in many areas simply not accessible to the alternative sources.

In the nanosecond regime, though, the pulsed laser has provided a unique capability to create, and control, extreme conditions of temperature gradients and interface motion which was not otherwise

obtainable. Temperature gradients and thermal quench rates for pulsed laser melting are typically three orders of magnitude greater than the highest rates obtained by splat cooling. Additionally, the laser allows almost unlimited flexibility in tailoring these gradients through the choice of wavelength (300 nm to 10 μm) and pulse duration (100 fs to 100 ns).

Detailed studies of many rapid quench phenomena were unfortunately, limited by the availability of experimental probes for monitoring the laser melts on these short time scales. For studies of the phase transformations in silicon, optical probes, such as surface reflectivity, were initially the only techniques capable of providing time resolved information on the melt behavior. Auston et.al. [9] first monitored this surface reflectance to confirm that the annealing process in Si occurred by melting and resolidification of a thin surface layer. Recently, Yen et.al. [10] have extended these surface reflectivity measurements to the sub-picosecond time regimes to obtain information on the transfer of energy from the electronic system to the phonon system in Si under intense radiation.

The surface reflectivity measurements suffer, though, from a lack of depth sensitivity since the reflectance is determined within the first few absorption lengths of the surface, typically 5-10 nm for metallic surfaces. Thus while the measurements can be extremely sensitive to phase changes on the surface, these measurements are able to determine very little of the melt kinetics within the bulk material. Alternative optical probes, using for instance the absorption through a sample or X-ray scattering, are being developed to provide depth and temperature information [11-12].

During the past two years, a time dependent and depth sensitive probe of the laser melting of Si has been developed [13-18]. This probe exploits the thirty fold electrical conductivity increase accompanying the transformation of Si from a semiconducting solid to a metallic liquid [19]. Monitoring of the transient electrical conductance provides a direct measurement of the volume of liquid present during laser irradiation. The first of these transient conductance traces, obtained in collaboration with R. B. Hammond, P. S. Peercy and G. J. Galvin, are shown in fig. 1.1. For large energy densities, the current flowing through a Au doped Si sample during irradiation was observed to increase due to the highly conducting liquid layer on the surface. As the surface resolidified, the current decreased proportionately providing a time resolved measure of the liquid thickness. In the figure, the cross hatch area of the curves indicate the conduction due to photo-generated carriers in the remaining solid Si.

While the data in fig. 1.1, due to the large photoconductivity response, allowed observation of the resolidification only, the use of silicon on sapphire (SOS) reduced this photoconductive signal dramatically and allowed detailed study of the entire melting and resolidifying process. For the first time, interface velocities and peak melt depths could be directly obtained and compared with theoretical models. This allowed a number of interesting questions to be addressed concerning the melting of Si.

First, the measurements allow comparison of the melt kinetics with various numerical models for the heat transport. Since the transfer of energy from the laser radiation to the Si sample occurs through the electronic system, it was suggested that non-thermal processes may play a

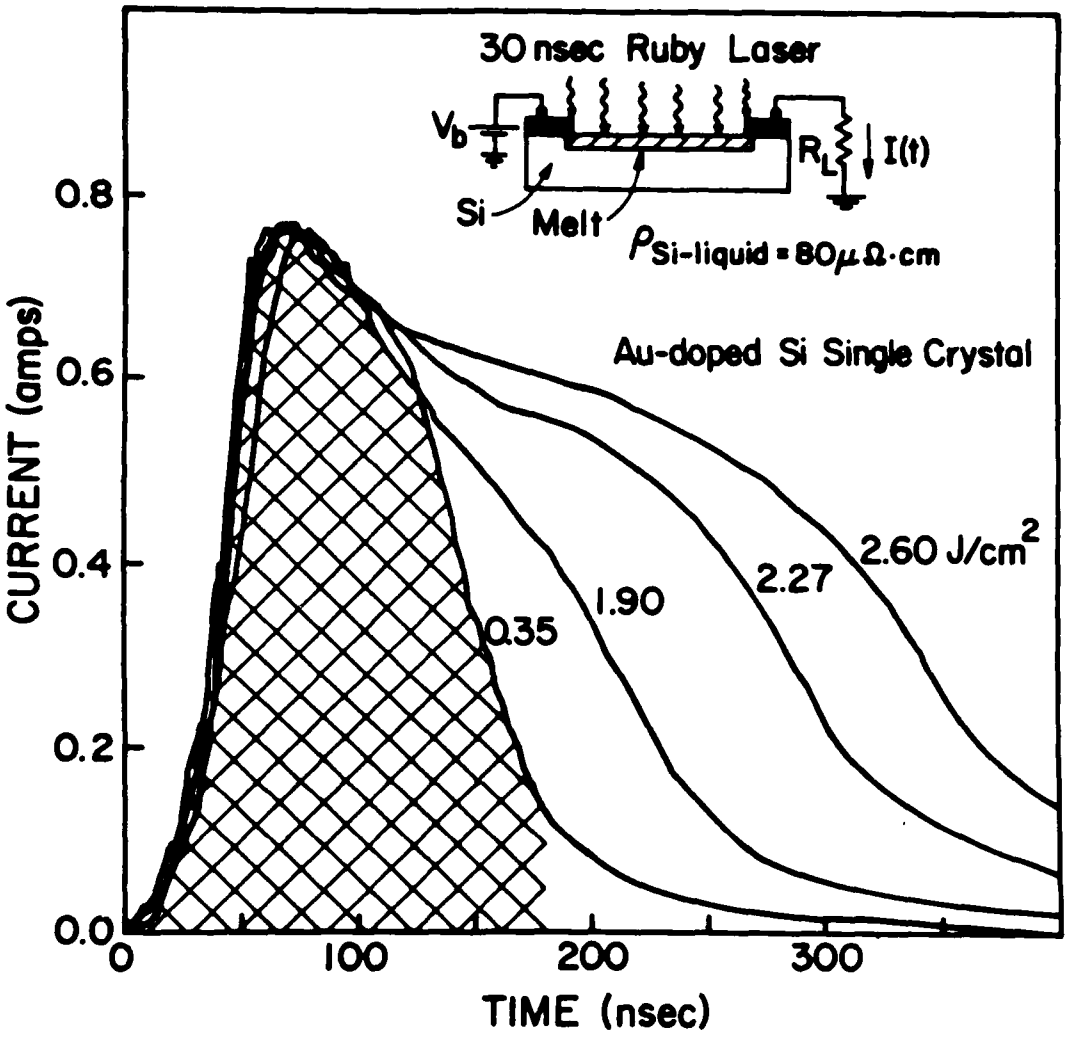

Fig. 1.1 The current versus time for Au-doped Si single crystal at various laser powers is shown. The cross hatch area represents the photoconductive response. The inset shows show a schematic drawing of the experiment.

significant role in describing the behavior of laser melts [20]. During irradiation at 30 ns, the melt kinetics have been studied in detail using the transient conductance technique with SOS. These melt kinetics were compared with both detailed numerical simulations and simple analytic estimates, based on normal thermal heat transport, and were shown to agree quite well. No large deviations were observed, suggesting that any non-thermal processes are insignificant on the nanosecond time scale.

Second, lasers allow study of the amorphous phase of Si at high temperatures. Under normal conditions, temperatures in excess of 600°C are difficult to obtain for amorphous Si due to the solid phase recrystallization. The rapid energy deposition of lasers allows high temperatures to be achieved with minimal recrystallization. Thermodynamic measurements indicate that amorphous Si will melt at a temperature significantly reduced from the crystalline melting point [21]. However, measurements of the solid phase epitaxial regrowth velocity at high temperatures using a CW laser have failed to confirm this melting temperature reduction [22]. The pulsed laser provides another method of studying the thermodynamics of amorphous Si at high temperatures. Using the transient conductance technique, direct observations of the transformation between amorphous Si and the liquid phase were made. By monitoring the kinetics of these melts, the reduction of the amorphous melting temperature, relative to the crystalline phase, was confirmed and a value of 200 ± 50 K was determined.

Additionally, observations of the melt behavior in amorphous Si at low incident energy densities identified the occurrence of an explosive crystallization event. The transformation of amorphous Si to poly crystalline Si at these low energy densities proceeded primarily by this

explosive crystallization process. The micro-structure of the resulting poly crystalline layer was also correlated with the melt behavior.

Finally, the technique allowed observations of the reverse transformation from the liquid phase directly to the amorphous phase. Under extreme growth conditions, laser melted samples are known to resolidify as the amorphous phase [23-24]. The transformation occurs at a critical velocity which was determined from the transient conductance to be 15 m/s.

REFERENCES

1. I. B. Khaibullin, E. I. Shtyrkov, M. M. Zaripov and M. F. Galyatudinov, Sov. Phys. Semicond. 11, 190 (1977).

2. Laser Annealing of Semiconductors, J. M. Poate, J. W. Mayer, Eds. (Academic Press, New York, 1982).

3. See, for example, the proceedings of the Materials Research Society, Laser-Solid Interactions and Transient Thermal Processing of Materials, edited by J. Narayan, W. L. Brown and R. A. Lemons, (North Holland, New York, 1983).

4. M. Hanabusa and M. Suzuki in Laser and Electron Beam Interactions with Solids, edited by B. R. Appleton and G. K. Celler (North Holland, New York, 1982), p. 559.

5. M. von Allmen, in Laser-Solid Interactions and Transient Thermal Processing of Materials, edited by J. Narayan, W. L. Brown and R. A. Lemons, (North Holland, New York, 1983), pp. 691.

6. D. J. Lischner and G. K. Celler in Laser and Electron Beam Interactions with Solids, edited by B. R. Appleton and G. K. Celler (North Holland, New York, 1982), pp. 759.

7. B. Y. Tsaur, J. P. Donnelly, John C. C. Fan and M. W. Geis, Appl. Phys. Lett. 41, (1982).

8. J. A. Knapp and S. T. Picraux, in Laser-Solid Interactions and Transient Thermal Processing of Materials, edited by J. Narayan, W. L. Brown and R. A. Lemons, (North Holland, New York, 1983), p. 557.

9. D. H. Auston, C. M. Surko, T. N. C. Venkatesan, R. E. Slusher and J. A. Golovchenko, Appl. Phys. Lett. 33, 437 (1978).

10. R. Yen, C. V. Shank and C. Hirlimann, in Laser-Solid Interactions and Transient Thermal Processing of Materials, edited by J. Narayan, W. L. Brown and R. A. Lemons, (North Holland, New York, 1983), p. 13.

11. P. H. Buxbaum and J. Bokor in Laser-Solid Interactions and Transient Thermal Processing of Materials, edited by J. Narayan, W. L. Brown and R. A. Lemons, (North Holland, New York, 1983), p. 51.

12. B. C. Larson, C. W. White, T. S. Noggle and D. Mills, Phys. Rev. Lett. 48, 337 (1982).

13. G. J. Galvin, M. O. Thompson, J. W. Mayer, R. B. Hammond, N. Paulter and P. S. Peercy, Phys. Rev. Lett. 48, 33 (1982).

14. Michael O. Thompson, G. J. Galvin, J. W. Mayer, P. S. Peercy and R. B. Hammond, Appl. Phys. Lett. 42, 445 (1983).

15. Michael O. Thompson, J. W. Mayer, A. G. Cullis, H. C. Webber, N. G. Chew, J. M. Poate and D. C. Jacobson, Phys. Rev. Lett. 50, 896 (1983).

16. G. J. Galvin, M. O. Thompson, J. W. Mayer, R. B. Hammond, N. Paulter and P. S. Peercy, Phys. Rev. B 27, 1079 (1983).

17. Michael O. Thompson and G. J. Galvin, in Laser-Solid Interactions and Transient Thermal Processing of Materials, edited by J. Narayan, W. L. Brown and R. A. Lemons, (North Holland, New York, 1983), p. 57.

18. Michael O. Thompson, G. J. Galvin, J. W. Mayer, P. S. Peercy, J. M. Poate, D. C. Jacobson, A. G. Cullis and N. G. Chew, submitted Phys. Rev. Lett.

19. Liquid Semiconductors, V. M. Glazov, S. N. Chizhevskaya and N. N. Glagoleva, Eds. (Plenum Press, New York, 1969).

20. J. A. Van Vechten, R. Tsu and F. W. Saris, Phys. Lett. 74A, 422 (1979).

21. E. P. Donovan, F. Spaepen, D. Turnbull, J. M. Poate and D. C. Jacobson, Appl. Phys. Lett., 42, 698 (1983).

22. S. A. Kokorowski, G. L. Olson and L. D. Hess, J. Appl. Phys. 53, 921 (1982).

23. P. L. Liu, R. Yen, N. Bloembergen and R. T. Hodgson, Appl. Phys. Lett. 34, 864 (1979).

24. A. G. Cullis, H. C. Webber and N. G. Chew, in Laser and Electron-Beam Interactions with Solids, edited by B. R. Appleton and G. K. Celler (North Holland, New York, 1982), pp. 131-140.

V. Melt-Front Kinetics and Ion Beam Mixing

B. Phase Formation in Ion Mixed Metal-Metal Systems

(prepared by Liang-Sun Hung)

Introduction

Ion mixing in silicide forming systems has been extensively investigated (1, 2, 13). With ion irradiation of the near-noble elements on Si substrates, the mixed layer has a composition that is polycrystalline in microstructure and corresponds to a well defined phase. The silicide that develops at the metal/Si interface is the same as that which forms when the sample is subjected to thermal annealing (1, 2, 9).

Ion mixing experiments on metal-metal systems have not produced conclusive results. So far, few ion mixing experiments have been performed on metallic bilayers. For systems with thin films of Al in contact with Ni, Pd and Pt, backscattering measurements revealed the formation of equilibrium compounds. The composition of the compounds differed from those obtained by thermal reactions, in contrast to that found in silicide-forming systems (1). Multilayered samples have been extensively utilized with metal-metal systems. The unique feature of the multilayer configurations is that the average composition of the whole sample is fixed so that a uniform mixed layer is formed as a result of ion mixing. Ion irradiation of the multilayered samples generally led to the formation of a metastable phase with no evidence of intermetallic compound formation although phase diagrams indicate

the presence of equilibrium compounds (10). There has been considerable effort to explain amorphorization in irradiated metallic alloys. Liu et al. recently formulated a "structural-difference" rule to predict when such amorphous phase will occur (12). The rule states that an amorphous binary alloy will be formed by ion mixing of multilayered samples when the two constituents are of different crystalline structures. The rule was reported to hold for eight metal-metal binary systems, irrespective of their atomic size and electronegativities. However, a lack of systematic investigation in the systems where the two components are of the same structure precludes generalization at this time. Moreover, the physical meaning of the rule, if any, is uncertain. Summarizing the experimental observations, it is found that distinct differences exist between metal-Si and metal-metal systems and that the results obtained in metal-metal systems with different sample configurations have not been put in a consistent framework. There is no clear picture of why equilibrium compounds have not been observed by ion mixing in the multi-layered samples and how amorphorization takes place during ion mixing.

In this chapter we report experimental observations of ion-beam mixing in the three kinds of binary systems that exhibit distinct differences in thermodynamic and kinetic behaviors upon thermal annealing. In Al/Ni, Al/Pd, and Al/Pt systems, the equilibrium phase diagrams show the presence of several intermetallic compounds with limited terminal solubilities (14, 15). In Au/Ni and Au/Cu systems, the phase diagrams are characterized by the absence of intermetallic alloys although there are differences between the two systems (14). For instance, a

miscibility gap occurs in Au/Ni, whereas a complete series of solid solutions is formed at high temperature in Au/Cu. In the Al/Au system, the phase diagram predicts five stoichiometric compounds (14). All of them have been detected with the samples prepared by depositing the exact stoichiometry quantities of Au and Al (16). A noticeable interfacial reaction was found in the as-deposited sample, indicating appreciable atomic diffusion at room temperature. The objective of this work is to determine under what conditions metastable phases or equilibrium compounds can be formed. The influences of phase equilibrium on the formation and structure of metastable phases are also investigated based on the results observed on various systems.

2.2. Amorphous and Crystalline Phase Formation in Al/Ni, Al/Pd, and Al/Pt Thin Films

It has been suggested that an amorphous binary alloy will be formed by ion mixing of multilayered samples in which the two constituent metals are of different crystalline structure when the composition of the multilayered samples is fixed near a deep eutectic and away from equilibrium compounds or pure metals (12). This work addresses the question of the formation of amorphous phases when the two components of the binary systems are of the same crystalline structure (fcc). The Al/Pt, Al/Pd and Al/Ni systems with the same fcc metal structure and different intermetallic structures have thus been chosen as subjects for this study. The structure of the ion-induced alloys has been examined for multilayered samples with various compositions and for bilayered samples as well.

2.2.1. Ion Mixing of Multilayered Samples

In these experiments, special layer structures were employed. Multilayers, ∿40 mm long, 5 mm wide, of two atomic species were deposited in an oil-free system so that the thickness of each sublayer varied linearly from zero to a chosen maximum over the length of the sample with Al on one end of the samples and Ni, Pd, or Pt on the other end (see insert in Fig. 2.1). Typically we chose 100-150 Å as maximum thickness of each sublayer and five bilayers were deposited during each cycle. The total thickness matches the penetration depth of the Xe ions used for ion mixing. As for substrates, in most cases cleaved NaCl crystals, damaged with neutrons, were used for transmission electron microscope (TEM) studies. When only Rutherford backscattering experiments (RBS) were planned, fine polished graphite samples were used as substrates. The self-supporting films were made by dissolution of the NaCl substrates in de-ionized water, and picked up on TEM grids for further treatments. Some samples on NaCl substrates were annealed and irradiated before being removed from the substrates and placed on TEM grids. For both procedures, the same results were obtained. The size of the films on the grids was chosen such that the average composition varied by about 8% from one specimen to the next. Moreover, the whole range of the composition could be investigated by using selected area diffraction techniques (SAD). Thermal annealing was performed in a vacuum furnace at pressure of 1×10^{-7} Torr. Ion mixing with 500-keV Xe ions was carried out at room temperature in a vacuum better than 1×10^{-6} Torr. The composition of the as-deposited samples

and the extent of ion mixing were determined by RBS and the crystalline structure of the binary alloys by TEM.

The as-deposited films of Al/Pt were examined with TEM and a sequence of lines due to both Al and Pt appeared in the diffraction patterns. The samples were then preannealed at 350°C for 1 h and TEM diffraction revealed the presence of several equilibrium compounds, as indicated in the Al-Pt phase diagram. Figure 2.1 shows one set of SAD patterns; the lattice spacings agree within 1% of data in ASTM tables.

Irradiation of the preannealed samples with 500 keV Xe to a dose of 2×10^{14} ions cm^{-2} produced a transformation of the equilibrium compounds to an amorphous phase for all of the Pt-Al binary alloys. The same behavior was found by direct ion mixing (without preanneal) of the multilayer samples. Backscattering showed that the layers were well mixed by a dose of 2×10^{14} Xe ions cm^{-2} and the diffraction patterns exhibited a strong diffuse band due to the formation of amorphous alloys over a wide (10%-90%) range of composition. The crystalline structure remained unchanged on samples with Al-rich or Pt-rich (> 90%) compositions.

In the Al/Pd system, the equilibrium phase diagram shows the presence of four compounds (Fig. 2.2). Preannealing the alternating layers of Pd-Al resulted in the formation of all the equilibrium compounds. After subsequent implantation with Xe at a dose of 2×10^{14} ions cm^{-2}, TEM measurements were performed to determine the change in the crystalline structure for those alloys. It is found that PdAl is insensitive to ion bombardment and remains crystalline even to a dose of 2×10^{15} ions cm^{-2}, while the phases $PdAl_3$ and Pd_2Al becon

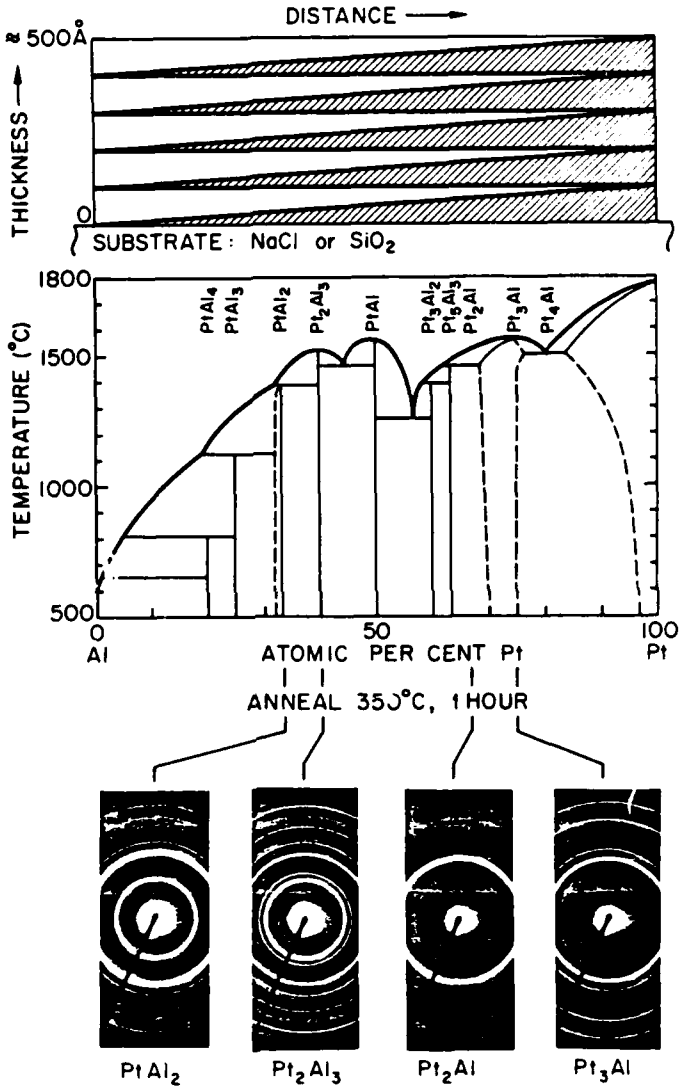

Figure 2.1. TEM diffraction patterns of the multilayered Pt/Al samples annealed at 350°C for 1 hr. showing the formation of the single-phase alloys indicatedby the equilibrium phase diagram. The top part of the figure represents schematically the structure of the samples.

amorphous. It is interesting to note that a diffuse band and a sequence of rings identified as PdAl reflection are present in the diffraction patterns of the original Pd_2Al_3 alloy (Fig. 2.2), which means the decomposition of the alloy Pd_2Al_3 to the PdAl and an amorphous phase. The results of ion mixing on the as-deposited samples are quite consistent with the above observations. The amorphous state is found in most samples. However, the equilibrium compound PdAl can be observed, if the compositions of the films lie in the neighborhood of PdAl or Pd_2Al_3.

The effects of ion beam bombardment in the Al/Ni system are similar to those found in the Al/Pd system. Upon irradiation to a dose of 2×10^{14} ions cm^{-2}, $NiAl_3$ was amorphorized, while NiAl retained its crystalline structure. The stability of NiAl under irradiation has previously been demonstrated with 2.5-MeV Ni ion bombardment. The transformation of Ni_2Al_3 to the Ni'l crystalline phase plus amorphous mixtures has also been observed as in the case of Pd_2Al_3. We found that Ni_3Al did not become completely amorphous; several faint lines are present in the diffraction patterns after irradiation with 2×10^{15} ion cm^{-2}. The SAD pattern in Fig. 2.3 shows the change in the crystalline structures for the different compounds after 2×10^{15} Xe cm^{-2} implant at 500 keV. For direct ion mixing of the multilayer samples without preanneal, TEM diffraction showed that only the intermetallic phase NiAl could be readily formed. The formation of NiAl has also been found for an Al single crystal implanted with Ni, followed by pulsed e-beam annealing (17). Crystallites of AlNi were observed in an amorphous matrix without trace of the other crystalline compounds.

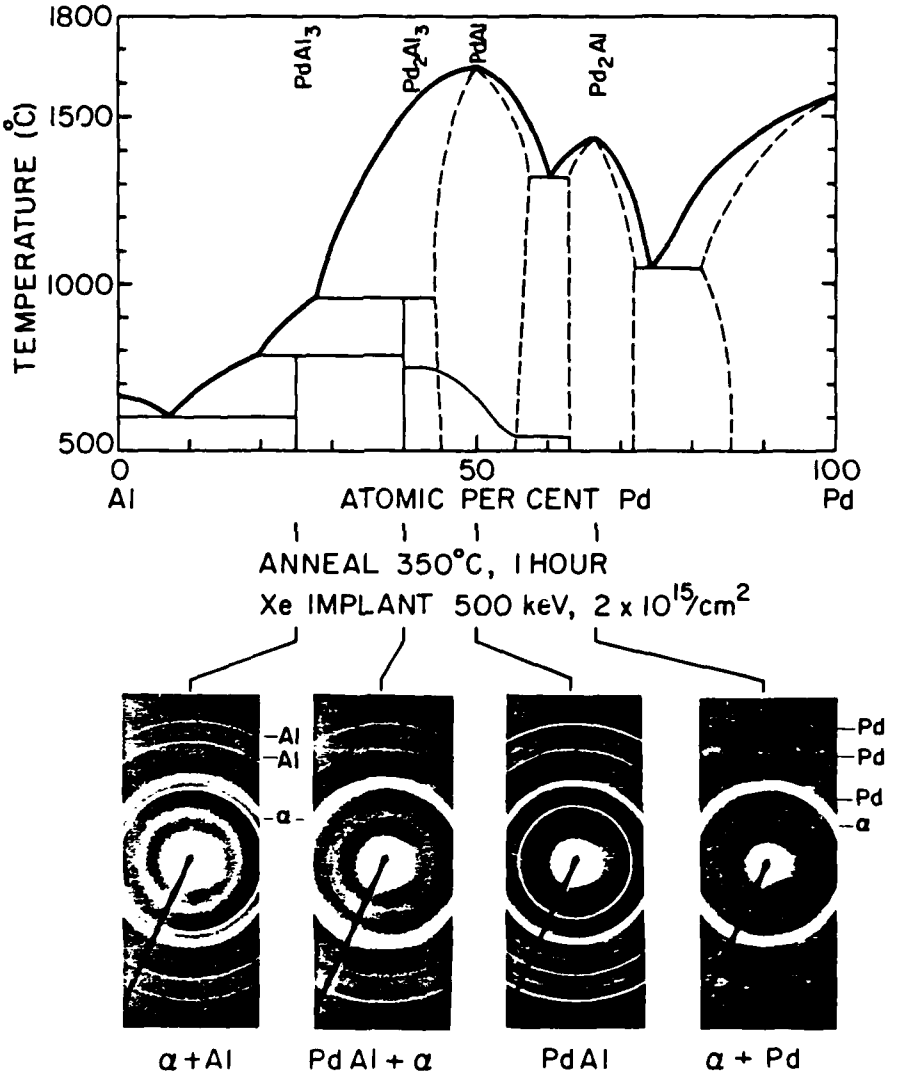

Figure 2.2. TEM diffraction patterns of the multilayered Pd/Al samples annealed at 350°C for 1 hr., followed by 2×10^{15} Xe cm^{-2} implant, indicating the transformation of the original Pd_2Al and $PdAl_3$ alloys to the amorphous phases and the Pd_2Al_3 phase to the PdAl phase.

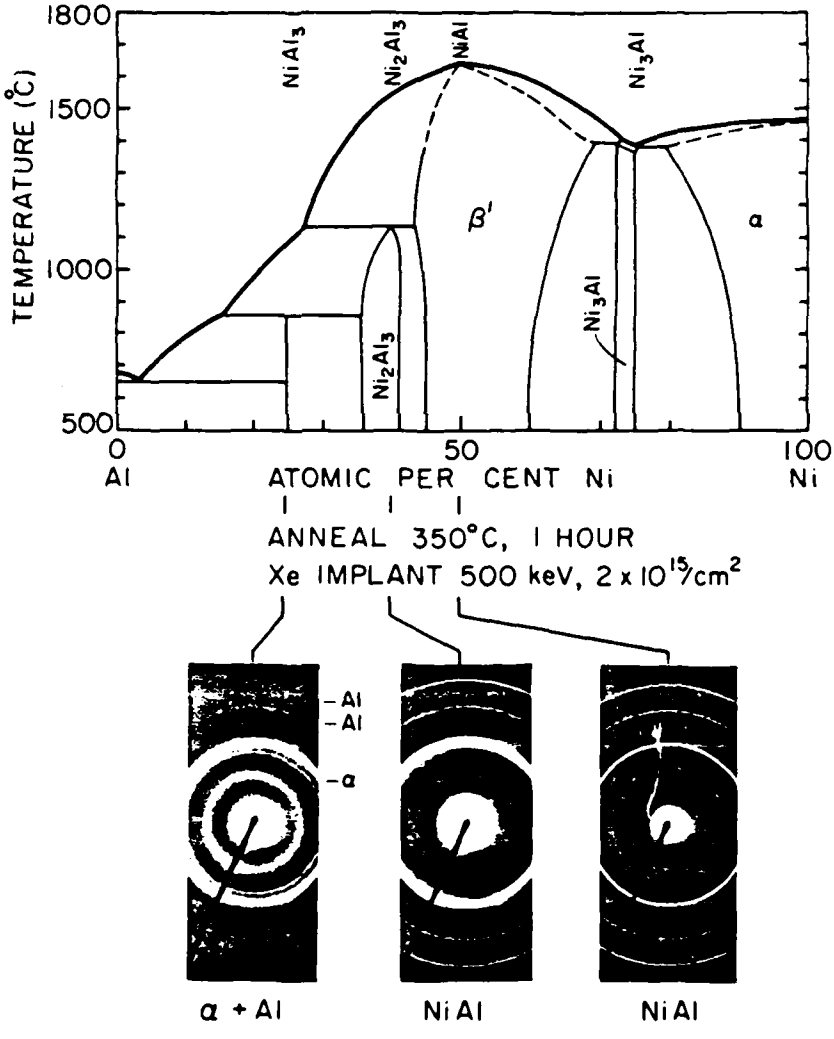

Figure 2.3. TEM diffraction patterns of the multilayered Ni/Al samples preannealed at 350°C for 1 hr., followed by 2×10^{15} Xe cm^{-2} implant, showing the formation of the amorphous or the crystalline NiAl phase, depending on the original compounds.

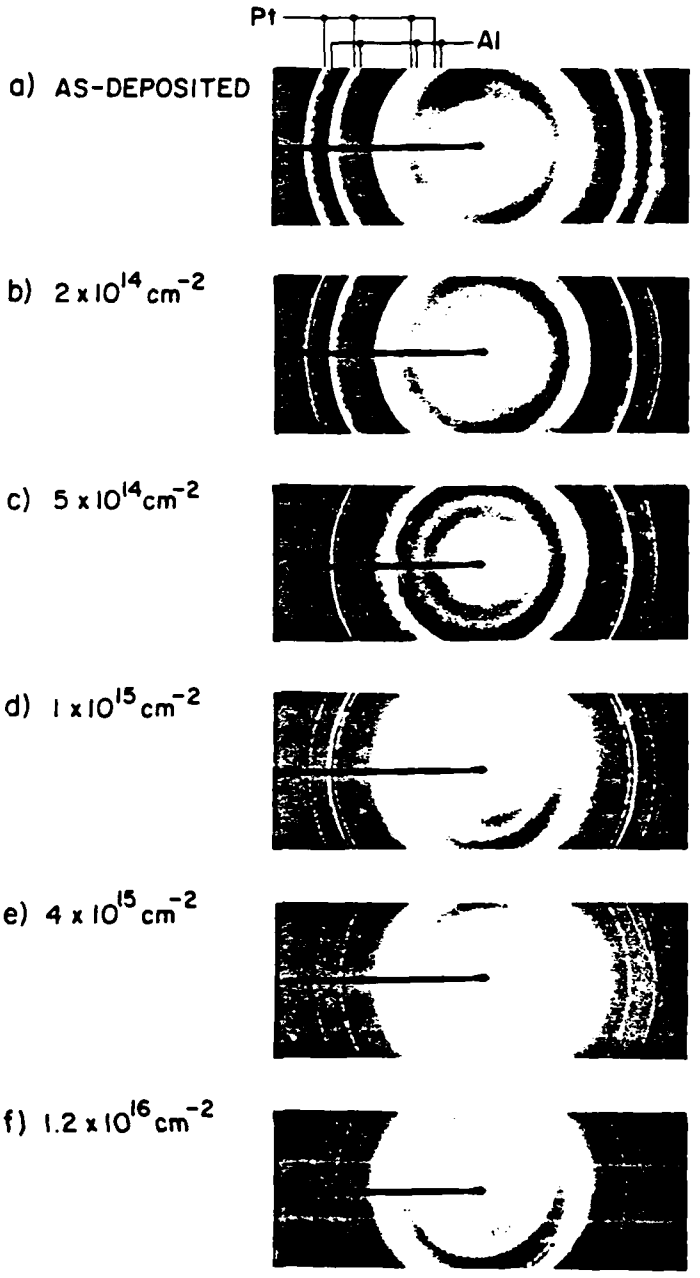

Figure 2.4. TEM diffraction patterns of the Pt/Al bilayers irradiated with Xe ions at doses ranging from 2×10^{14} to 1.2×10^{16} ions cm^{-2}, showing no trace of crystal compounds.

2.2.2. Ion Mixing of Bilayered Samples

RBS spectra taken from ion mixed Pt/Al bilayers showed signs of step evolution as early in dose as 2.5 x 10^{14} Xe ions cm^{-2}. Electron diffraction examination of mixed bilayers revealed the presence of 2 diffuse bands in addition to signs from Pt and Al in the diffraction pattern. As the dose was increased the intensity of the diffuse band was also found to increase while the Pt diffraction intensity decreased. Further increases in dose resulted in the total attenuation of the Pt signal and only diffraction from Al and an amorphous phase was observed (Fig. 2.4). This condition persists up to the final dose of 12 x 10^{15} Xe ions cm^{-2}. There is no evidence for the presence of crystal compounds.

Electron diffraction patterns taken of Pd/Al bilayer samples irradiated with ion doses ranging from 5 x 10^{14} cm^{-2} to 12 x 10^{15} cm^{-2} revealed that the only crystalline phase formed was PdAl. The formation of the compound PdAl took place at the lowest mixing dose used. With a further increase in dose, the attenuation of the Pd signal and the development of a diffuse ring were observed. In addition, reflections from PdAl and Al were still present in the diffraction patterns.

When ion mixed samples of Al/Ni bilayers were examined by electron diffraction it was found that the only ion induced crystalline compound present was NiAl. Diffraction confirmed the presence of this intermetallic compound at doses ranging from 1 x 10^{15} to 12 x 10^{15} ions cm^{-2}. At a dose of $\sim$ 6 x 10^{15} ions cm^{-2} a diffuse band appears in the diffraction pattern indicating the presence of an ion induced amorphous

phase. Both the amorphous and NiAl phases were observed by diffraction up to the maximum dose.

2.2.3. Discussion

The effect of ion mixing on multilayered samples in a metal-metal system is strongly correlated with the sensitivity of the equilibrium compounds to ion beam bombardment. An explanation for the observed variation in the behavior of the alloys is suggested by a comparison of their crystalline structures. Table 2.1 gives the crystallographic data on the binary alloys in the three systems (18).

Based on this comparison we would attribute the difference in radiation sensitivity to the difference in the crystal structure of the alloys. As an example, PdAl and NiAl are simple cubic structures with two atoms in the unit cell, and are able to survive under ion irradiation. The phase Ni_3Al did not become completely amorphous; it has four atoms per unit cell. The other, more complex, structures became amorphous.

With ion irradiation of bilayered samples the system is free to seek a possible preferred composition for the mixing region as compared to the multilayered samples in which the average composition is fixed by the relative thickness of the respective layers of the constituents. From this consideration one would expect that the result of ion mixing in bilayers might differ from that in multilayers. The present investigations clearly demonstrate that the outcome of ion mixing is constrained by the process itself, independent of the sample configuration.

Table 2.1. Crystalline structure of the binary alloys in Al/Pt, Al/Pd and Al/Ni systems

Al/Pt Compound	Structure	Al/Pd Compound	Structure	Al/Ni Compound	Structure
Al_2Pt	cF_{12}	Al_3Pd	oP_{16}	Al_3Ni	oP_{16}
AlPt	cP_8	Al_3Pd_2	hP_5	Al_3Ni_2	hP_5
Al_3Pt_5	oP_{16}	AlPd	cP_2	AlNi	cP_2
$AlPt_3$	tP_4	$AlPd_2$	oP_{12}	$AlNi_3$	cP_4

Remarks: c, h, o, and t refer to cubic, hexagonal, orthorhombic, and tetragonal. F and P refer to all face centered and primitive. Numbers refer to the number of atoms in the unit cell.

The ion-induced amorphorization process is thought to occur as follows. As ions penetrate into the sample, the kinetic energies are rapidly deposited in a local region surrounding the ion track. This nonequilibrium localized zone with highly energetic atoms is considered to quench to the lattice temperature rapidly after the collision cascade (19). During this relaxation period atoms attempt to rearrange themselves. If the relaxation time is sufficient for precipitates to nucleate, crystalline phase formation may be achieved. The time required for nucleation is strongly influenced by the temperature, the crystalline structure of nuclei and the composition of the films which have been homogenized with thermal treatments or ion beams. If the overall composition is not close to that of the compound with a simple crystalline structure and there is not a strong chemical driving force to promote a significant atomic motion, crystalline phase formation may be inhibited.

2.3. Extension of Solid Solubilities in Au/Ni and Au/V Bilayers

Previous observations (11) on ion mixing of multilayered samples consisting of two elements showed that in the Au-Ni system, single phase fcc solid solutions over an entire range of composition have been produced and that in the Au-V system, the Au-rich alloys exhibited a fcc structure while the V-rich alloys exhibited a bcc structure. In the present work, we report experimental observation of ion-beam-mixing in Au/Ni and Au/V bilayers.

2.3.1. Ion Mixing of Au and Ni

We deposited Au and Ni on SiO_2 substrates sequentially, then irradiated the samples with Xe ions. At a dose of 1×10^{15} cm^{-2}, a change in slope at the interface edge of Au and Ni profiles in the backscattering spectrum revealed that intermixing began to develop. With increasing dose, both the slopes and the heights of Au and Ni signals progressively reduced, indicating continuing penetration (Fig. 2.5). After bombardment to a dose of 6×10^{15} cm^{-2}, Au and Ni were totally mixed with a graded composition and a distribution of Au out to the free surface. X-ray analysis showed broadening of reflections at the positions corresponding to that from pure Au and Ni, indicating the formation of solid solutions with various compositions (Fig. 2.6). The removal of Ni by sputtering could be clearly seen by the shift of the Si spectrum to higher energy. The TEM observations were consistent with x-ray diffraction and backscattering measurements. The samples were investigated with TEM using selected area diffraction techniques. As the ion dose is increased, the diffraction rings of Ni and Au undergo broadening indicating the incorporation of Au into the Ni lattice and vice versa.

The equilibrium phase diagram of Au-Ni shows that Au and Ni are completely soluble at temperatures above 800°C, but a miscibility gap exists at low temperatures. The production of continuous series of solid solutions in the present study with bilayers combined with the previous results obtained in ion mixing of Au/Ni multilayers indicates that ion mixing can overcome the constraint of miscibility between two elements irrespective of the sample configuration.

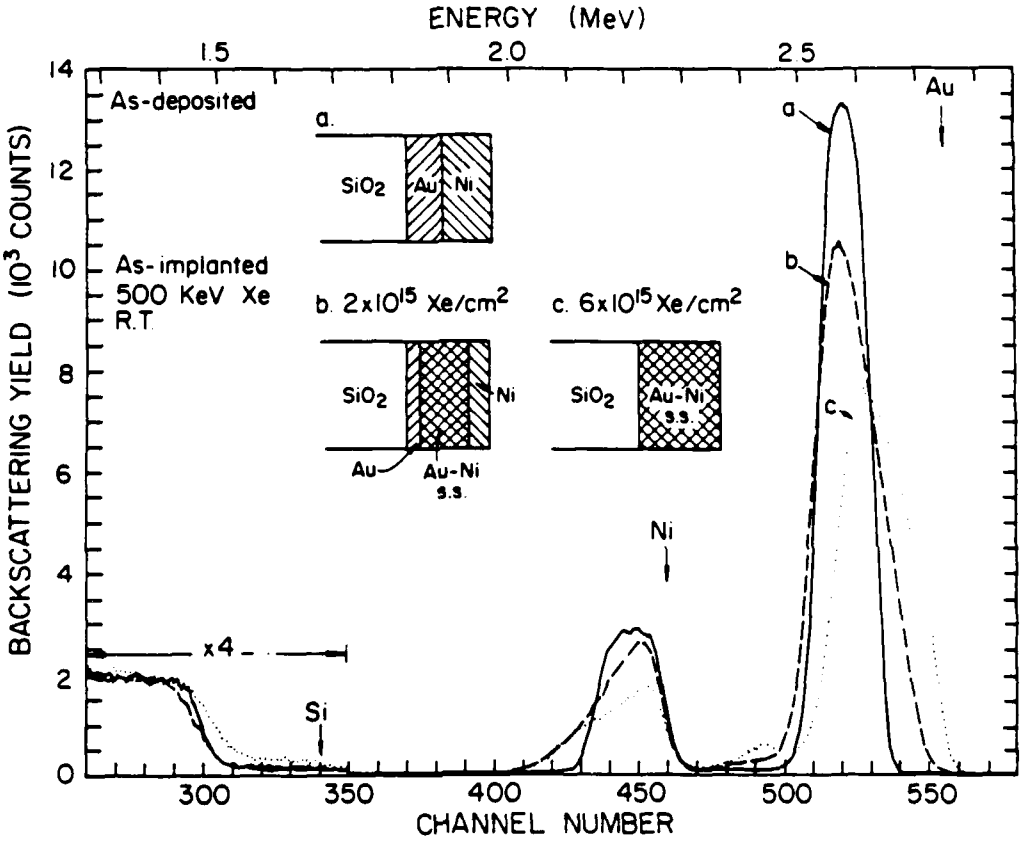

Figure 2.5. Ion backscattering spectra for SiO_2/Au/Ni samples bombarded with 500 keV Xe ions to various doses. The amount of intermixing increases with ion doses. After bombardment to a dose of 6×10^{15} cm^{-2}, Au and Ni are totally mixed with a graded composition.

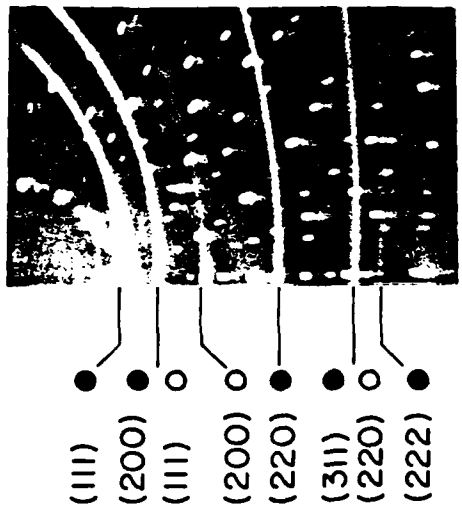

a. As-deposited

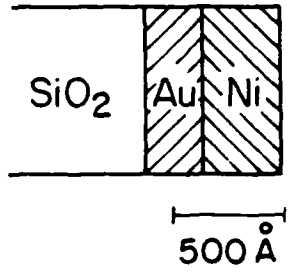

● Au

o Ni

b. As-implanted
500 KeV Xe
6×10^{15} cm^{-2}
R.T.

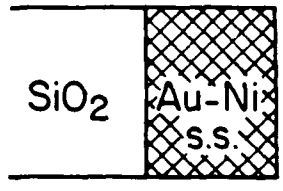

Figure 2.6. X-ray diffraction patterns for Au/Ni bilayers on SiO_2 before and after bombardment with 500 keV Xe ions to a dose of 6×10^{15} cm^{-2} showing the formation of solid solutions with various compositions by ion mixing. For irradiated samples the broadening of reflections at the positions corresponding to those from pure Au and Ni is observed.

2.3.2. Ion Mixing of Au and V

We deposited Au and V on SiO_2 or NaCl substrates sequentially, then irradiated the samples with Xe ions. The thickness of the samples was designed to be approximately equal to the value of Rp + 2ΔRp of the irradiated ion. Rp is the projected range of the ion and ΔRp is the standard deviation. RBS spectra showed continuing intermixing of the two elements with increased doses. Electron diffraction patterns taken of bilayers reacted with ion doses ranging from 2×10^{15} cm^{-2} to 1×10^{16} cm^{-2} revealed no traces of equilibrium compounds. The formation of solid solutions was observed at the lowest mixing dose used. The original V diffraction rings shifted toward the central spot while the Au rings shifted in the opposite direction (Fig. 2.7). As the ion dose was increased, the diffraction rings were progressively displaced. At the same time, continuing attenuation of the diffraction signals occurred due to the removal of Au and V by sputtering.

The phase diagram of Au-V is markedly different from that of Au-Ni. Three ordered phases are present with compositions centered around Au_4V, Au_2V, and AuV_3. In this work, fcc solutions were formed with the lattice parameters slightly smaller than that of pure Au due to the incorporation of V into the Au lattice. Simultaneously, bcc solutions were produced with the lattice parameters slightly larger than that of pure V due to the incorporation of Au into the V lattice. The results are consistent with that reported by Tsaur et al. (11), who found with ion mixing of Au/V multilayers, supersaturated fcc and bcc solutions were obtained without forming the ordered phases.

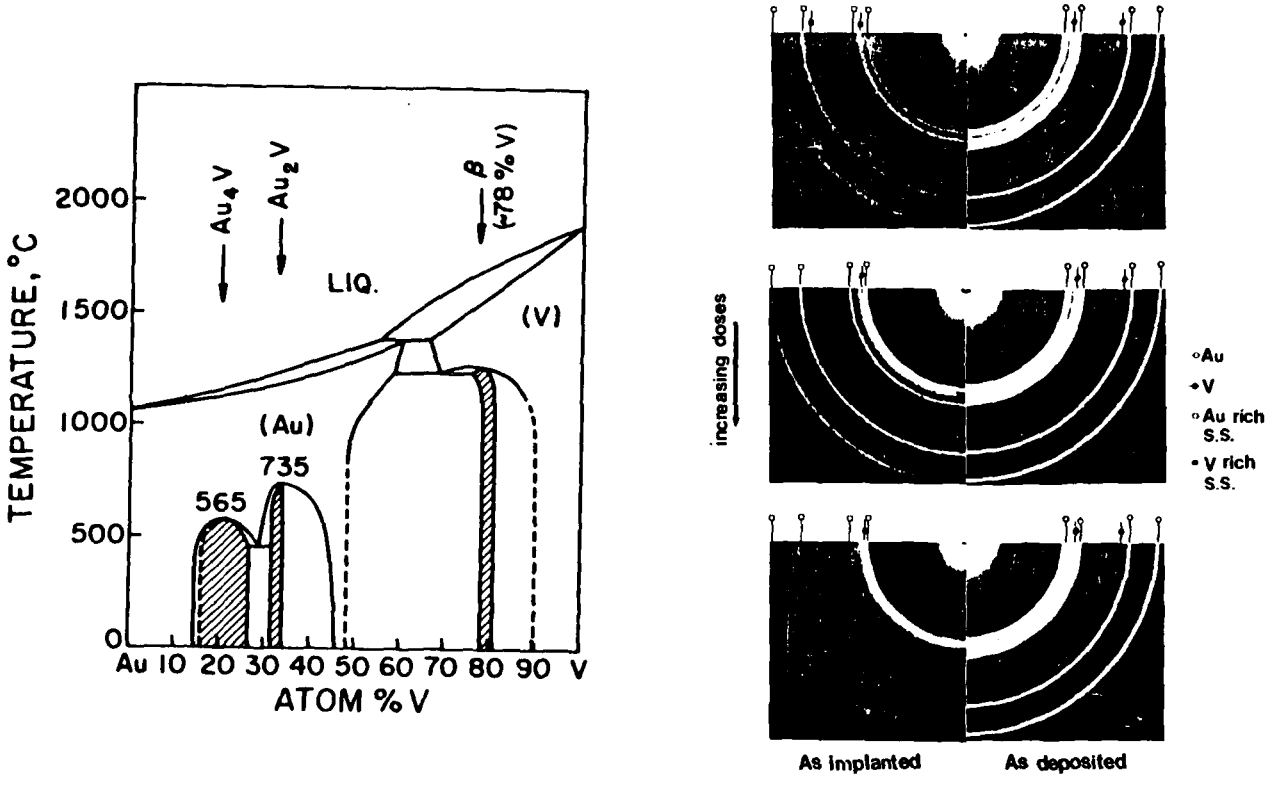

Figure 2.7. a) Equilibrium phase diagram of Au-V. b) TEM diffraction patterns of the Au/V_2 bilayers irradiated with Xe ions at doses ranging from 2×10^{15} to 1×10^{16} ions cm^{-2}, showing the presence of Au-rich and V-rich solid solutions without ordered compounds in the mixed layers.

The constitution diagram shown in Fig. 2.7 indicates that the Au solid solution extends from pure Au to about 52 at. % Au and the ordered compounds of Au_4V and Au_2V are formed at temperatures of 565 and 735°C respectively by a disorder-order transition (20). Ion mixing of Au and V with multilayered or bilayered samples produced the fcc solid solution with no evidence for the presence of the ordered phases. As ion irradiation is a non-equilibrium process, the atomic distribution in a mixed layer is likely to be random in nature. The formation of a disordered solid solution is kinetically more favorable than that of an ordered phase, because the latter requires a high atomic mobility.

For multilayered samples with a composition $Au_{25}V_{75}$, a bcc solid solution was observed. Similar results were recently found in the quenched alloys, where V-rich solid solution was produced with a broad composition range from pure V to 68 at. %V (21). The kinetics of the transformation from the quenched metastable solid solution (α phase) to the intermetallic compound corresponding to the approximate composition AuV_3 (β phase) were studied by means of electrical resistivity measurements. The transformation began at 600°C, while the β phase transformed to the α phase at 1280°, which was then stable up to the solidus. This experiment provided experimental data to determine a new equilibrium phase diagram as shown in Fig. 2.7. From the new phase diagram, one would expect that thermodynamics favors the production of solid solution rather than that of amorphous mixtures, when the formation of the β phase is kinetically suppressed. This is indeed the case, as we found in the mixing of Au and V.

2.4. Ion Induced Solid Solution and Ordered Compound Formation in Au/Cu Bilayers

In the present study we have investigated the ion beam mixing of Au/Cu bilayers. The equilibrium phase diagram in the Au-Cu system shows that a complete series of solid solutions is formed at high temperature, and that several ordered compounds exist at low temperature all of which have been extensively studied in thermal annealing (14). Au-Cu solid solutions have previously been produced by direct implantation of Au into single crystal Cu or by ion mixing of Au films with single crystal Cu substrates (22, 23). The concentration of Au at peak of the distribution is about 10 at. %. Considerable efforts have been put into the study of ordering-disordering transitions by electron and neutron bombardment using electrical resistivity measurements (24-26). The purpose of the present work is to investigate the possibility of producing ordered compounds by ion mixing. Our approach is to study the effect of the temperature and ion species on the mixing of Au/Cu bilayers. The polycrystal bilayers were used for investigating the amount of mixing versus ion dose and the single crystal bilayers for studying the formation of solid solutions and ordered compound in the Au-Cu system.

2.4.1. Experimental

Thin bilayers of polycrystal Au and Cu were sequentially evaporated onto SiO_2 substrates at a pressure of $\sim 5 \times 10^{-7}$ torr. The total thickness of the bilayers was roughly equal to $Rp + 2\Delta Rp$. Energetic Xe ions were employed with doses ranging from 1×10^{15} to 8×10^{15} ions cm^{-2}. The samples were held on the sample holder by a thin

layer of heat sink compound to ensure adequate thermal contact. The current densities were kept at 0.5 μA cm^{-2} or below so that beam heating of the sample was negligible.

Single crystal bilayers of Au and Cu were prepared by the sequential deposition of Au and Cu onto NaCl single crystal substrates, which were previously damaged by neutron irradiation and cleaved prior to loading into the evaporation system. After evacuation to 1 x 10^{-6} torr, the substrates were heated to 350°C and Au layers 700 Å thick were deposited on the substrates. When the samples were cooled down to 50°C in the deposition chamber, Cu layers 700° Å thick were evaporated on top. The samples were then irradiated with 250 keV Ar ions at temperatures ranging from 20°C to 200°C. The temperature was monitored with a thermal-couple attached to the sample holder. The sample normal was misaligned against the beam by 7° to avoid channeling effects. To insure the reactions observed at high temperature are not caused by thermal effects, a control sample, which was mounted on the same heating stage but shielded from ion beam, was used to monitor the reaction induced by thermal heating. No detectable reaction was observed for the control samples in this experiment. Thermal treatments were carried out in situ using a TEM heating stage at a pressure better than 1 x 10^{-6} torr or in a vacuum furnace at pressure 1 x 10^{-7} torr.

2.4.2. Results

A. Polycrystal Au/Cu Bilayers

After irradiation of polycrystal bilayers with Xe, ion backscattering analysis revealed a change in slopes of the Au and Cu profiles (Fig. 2.8), indicating intermixing of Au and Cu. As the dose was increased, the slopes decreased. The depth profile of composition was plotted in Fig. 2.9 using the data from Fig. 2.8. It is clear that Au and Cu were totally mixed with a graded composition at a dose above 4 x 10^{15} ions cm^{-2}. The structure change of the samples at various stages of ion mixing were examined by x-ray diffraction. A broadening of the Au and Cu reflection lines was observed, thus indicating the formation of solid solutions with various compositions (Fig. 2.10). The amount of broadening increased with increased ion dose. TEM observations were consistent with x-ray diffraction and backscattering measurements. Selected area diffraction techniques showed that the diffraction rings of Au and Cu undergo progressively broadening with increasing doses. No other compounds were identified during the room-temperature mixing process. In irradiated samples annealed at 350°C for 1 hr, a crystalline phase was observed and identified as the ordered compound of CuAu.

B. Single Crystal Au/Cu Bilayers

The single crystal bilayers provide a suitable medium for the study of solid solutions and ordered compounds in this work. Single crystal bilayers were irradiated at room temperature with Ar ions of 250 keV. Intermixing of Au and Cu took place at a dose of 3 x 10^{15}

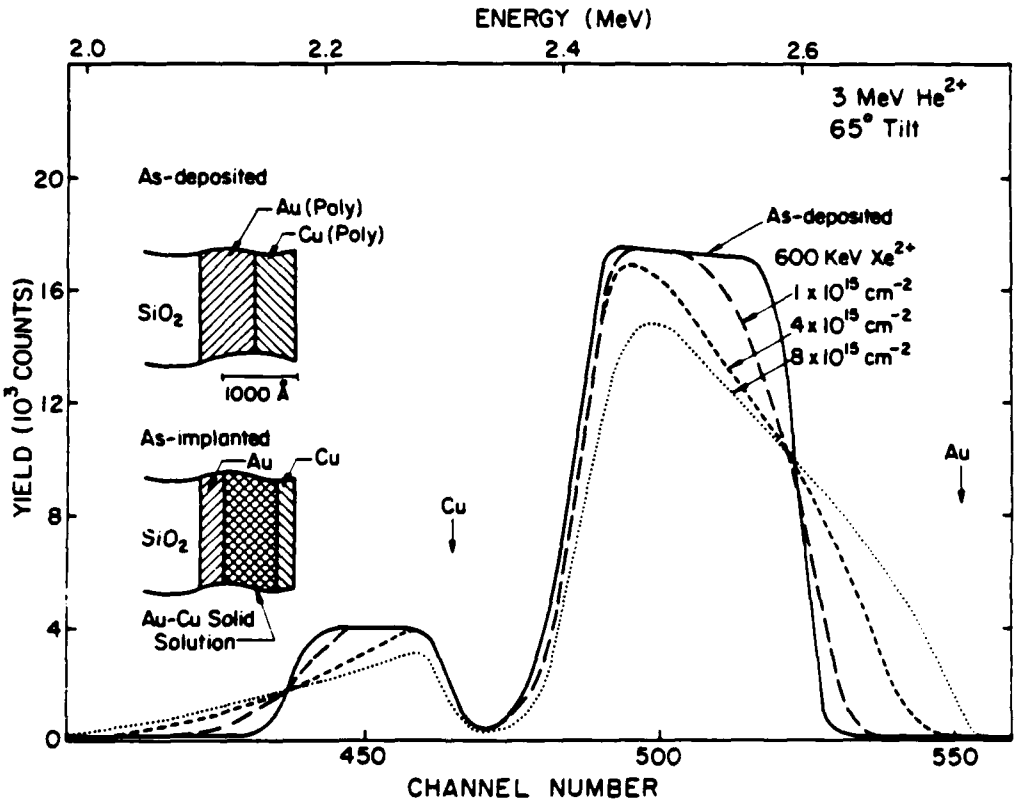

Figure 2.8. Ion backscattering spectra for SiO_2/Au(poly)/Cu(poly) samples bombarded with 600 keV Xe ions to various doses at room temperature.

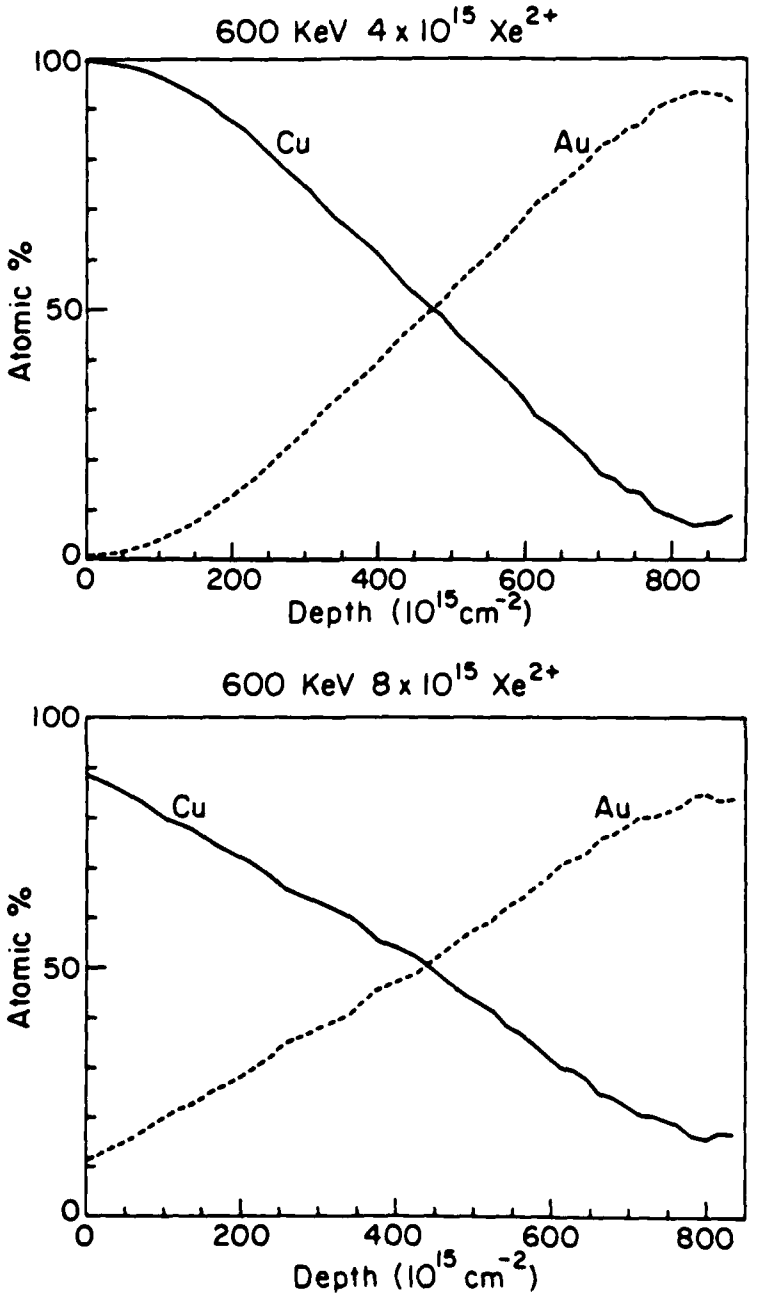

Figure 2.9. Depth profiles of the composition in the mixed layers for SiO_2/Au(poly)/Cu(poly) samples bombarded with 600 keV Xe ions to a dose of 4×10^{15} ions cm^{-2} and a dose of 8×10^{15} ions cm^{-2}.

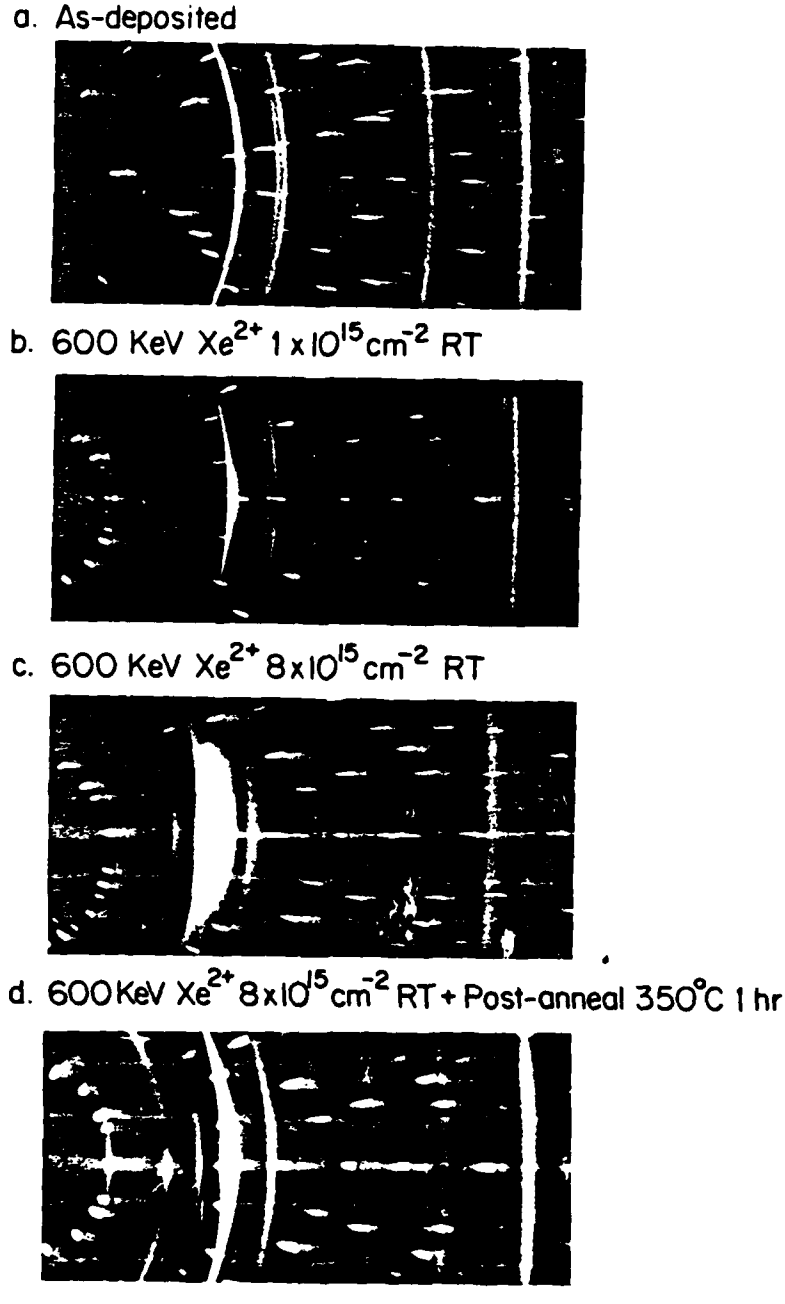

Figure 2.10. X-ray diffraction patterns for SiO_2/Au(poly)/Cu(poly) samples bombarded with 600 keV Xe ions to various doses at room temperature showing continuing broadening of the Au and Cu reflection lines. Annealing of the irradiated samples results in the transformation of solid solutions to the ordered compound of AuCu.

ions cm^{-2}, and continued to develop with dose. After bombardment to a dose of 3×10^{16} ions cm^{-2}, Au and Cu were completely mixed with a distribution of Au out to the free surface (Fig. 2.11). Electron diffraction examination showed that Au and Cu had formed substitutional solid solution (Fig. 2.12a). Subsequent heat treatment of the irradiated sample at 350°C for 1 hr resulted in the formation of an ordered compound as indicated by the presence of superlattice reflections in the diffraction patterns. These superlattice reflections have mixed khl indices which are not permitted for the fcc structure of the random Au-Cu solid solution. This transformation to an ordered compound was also observed when the bilayers were either irradiated with 250 keV Ar ions at 200°C or irradiated with Ar ions at room temperature followed by 50 keV He ions irradiation at 60°C (Fig. 2.12b). Annealing in situ using a TEM heating stage resulted in an increase in the intensity of the superlattice reflections. The results of annealing an irradiated sample at 350°C for 1 hr is illustrated in the diffraction pattern of Fig. 2.12c. The central spot corresponds to the undeviated beam; the four sets of intense fourfold satellite spots correspond to the (110) point of the fundamental reciprocal lattice, being split into four; the (020) spot is also surrounded by new spots. The fourfold satellite spots are typical for the superlattice CuAu with antiphase domain boundaries (27).

2.4.3. Discussion

Au-Cu solid solutions with a graded composition have been formed by irradiation of Au/Cu bilayers with Xe or Ar ions at room tempera-

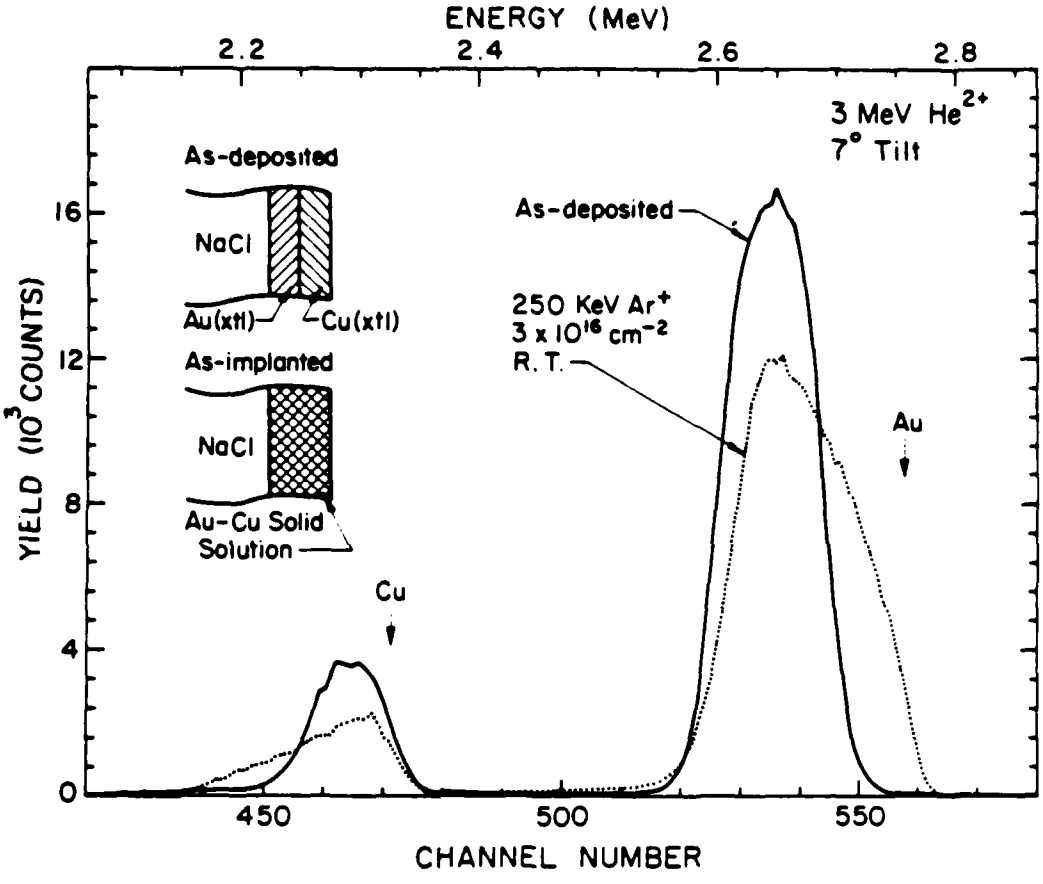

Figure 2.11. Ion backscattering spectra for the single crystal bilayer of Au and Cu irradiated with 250 keV Ar ions to a dose of 3×10^{16} cm^{-2} at room temperature.

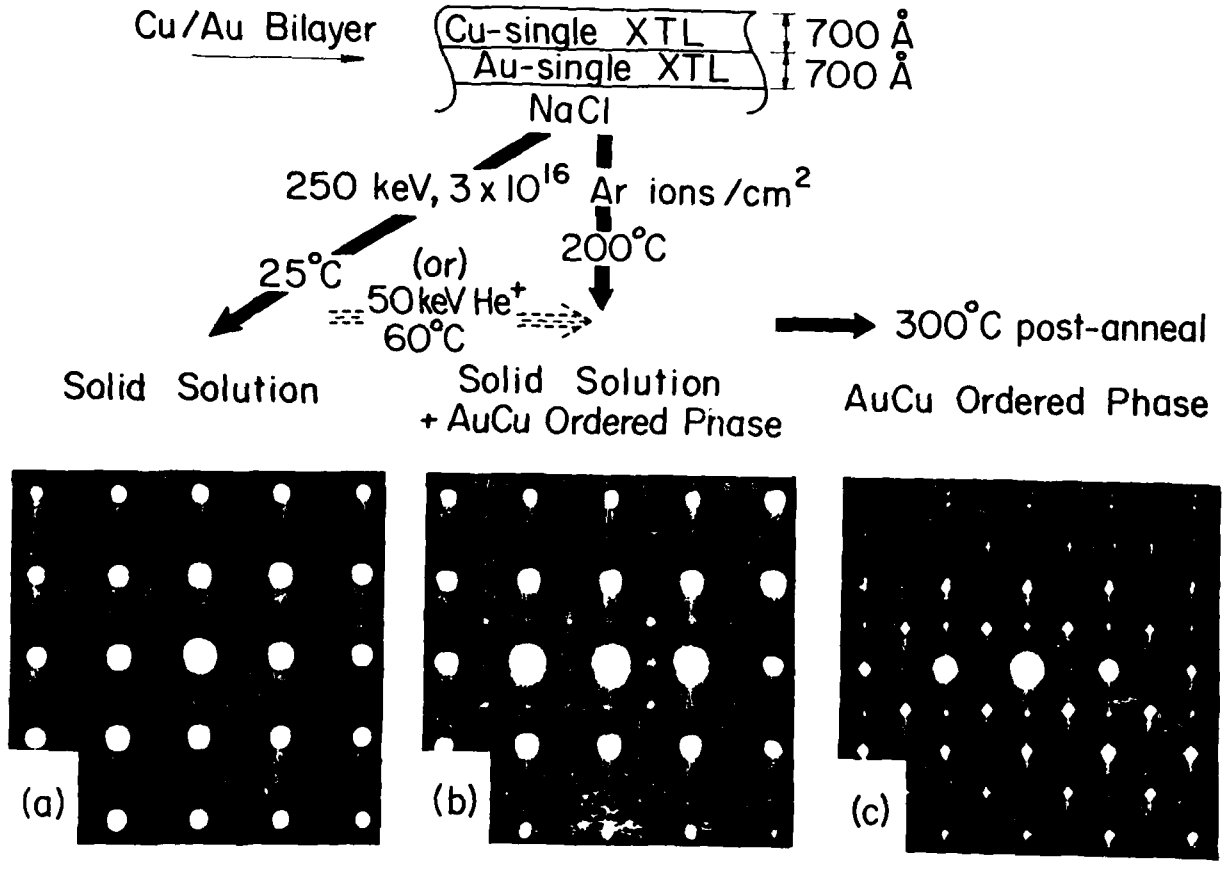

Figure 2.12. Transmission electron diffraction patterns for the single crystal bilayer of Au and Cu after various processing conditions.

ture. The previous investigation of ion induced reaction showed that the direct implantation of Au into single crystal Cu resulted in the formation of substitutional solid solution (22). A similar result has been obtained by the mixing of Au films on single crystal Cu substrates (23). The concentration of Au at the peak of distribution was about 10 at % and was mainly limited by sputtering. In this work the solubility was extended over the whole range of the composition by the mixing of Cu on Au.

In the present study, both x-ray diffraction and electron diffraction did not reveal any crystal compound in the mixed layers after the irradiation with Xe or Ar ions although the equilibrium phase diagram shows the presence of ordered compounds of Cu_3Au, CuAu, and $CuAu_3$. Similar results have previously been reported in ion mixing of Pt/Al bilayers, where Pt was gradually mixed with Al with no trace of intermetallic compound during Xe ion bombardment. A distinct difference in ion induced metastable alloys exists between the two systems. Au is mixed with Cu to form substitutional solid solutions, while Pt reacts with Al to form an amorphous mixture. These observations are closely related to the common features of ion mixing and the different thermodynamic behaviors in the two systems. Ion mixing can be considered as a rapid quench process within the framework of an energy spike model (28-30). In general, the time scale on which the energy spike occurs is smaller than that for nucleation of crystalline compounds with complex structures. Thus the formation of complex structured compounds is suppressed, as we found in the Au-Cu and Pt-Al systems. As long as the formation of ordered compound is

prohibited in Au-Cu, the extension of solubility by ion beam becomes energetically favored because Au and Cu are soluble at high temperature. As a result of ion mixing, substitutional solid solutions are formed. In contrast, the terminal solubilities in Al-Pt are limited to be about 1-3 at % even at high temperature. Although thermodynamics favor the formation of a compositionally segregated state containing Al-rich and Pt-rich solid solutions, the phase separation can not be achieved due to kinetic restriction, leading to the formation of amorphous mixtures. After the energy spike subsides, the presence of radiation induced defects can enhance atomic diffusion. However, atomic diffusion is not appreciable at room temperature (26), thus non-equilibrium states are retained in the Au-Cu and Al-Pt systems.

As radiation enhanced diffusion is a thermally activated process, appreciable atomic diffusion can occur at elevated target temperatures. Consequently, the as-implanted system acquires thermal equilibrium and equilibrium phases are formed. In this study when the implantation is performed with Ar ions at 200°C, the mixed atoms make a local redistribution to form an ordered compound with the aid of radiation induced defects at elevated temperature. The formation of an ordered compound has also been achieved by irradiation with Ar ions at room temperature followed by irradiation with He ions at 60°C. The temperature at which the formation of ordered compounds takes place depends on the mass of the bombarding ions due to the difference in the energy density deposited by ions (31). Under Ar ion irradiation, the defects were created within the cascade regions and become trapped. Then only few

defects contribute to the equilibrium phase formation, so that a high temperature is required for the ordered state to be established. Under He ion irradiation, the defects are created homogeneously. Thus a low temperature is sufficient for the local rearrangement of atoms. The transformation of substitutional solid solution to the ordered compound by He implantation follows the behavior noted in the long-range ordering under electron and neutron irradiation; when a partially ordered alloy was bombarded at a relatively high temperature, the electrical resistivity of the irradiated material drastically decreased (32).

2.5. Equilibrium Compound Formation by Ion Beams in Au-Al Bilayers and Multilayers

The phase diagram of the Au-Al system predicts five stoichiometric compounds, among which $AlAu_2$ and $AuAl_2$ have melting point maxima and all others form peritectically (14). Thermally induced reactions in the Au-Al system have been investigated (16). In the thin film couples, Al_2Au_5 is formed initially during deposition, then $AlAu_2$ forms and grows at temperature less than 100°C. Subsequent annealing results in the formation of various compounds depending on the relative quantity of material available. In the case where Al >> Au, the formation of Al_2Au is observed after all the Au has been consumed. The characteristic of the phase diagram is similar to that in the other Al-based systems where several intermetallic alloys exist with limited terminal solubilities, whereas the kinetics in the Au-Al system is uniquely featured by the high reaction rate at relatively low temperatures. The present investigation shows that the high atomic

mobility at room temperature greatly affects the phase formation by ion beams.

Samples were prepared by sequential deposition in an oil free vacuum system at pressure of 2×10^{-7} Torr. Multilayered samples were prepared by deposition of alternating Au and Al layers on NaCl substrates. The thickness of each sublayer was varied linearly from zero to 150 Å over the length of the sample with Al on one end and Au on the other end. The conventional bilayers were deposited on SiO_2 substrates.

A series of multilayered samples was prepared with various compositions and the structure of each sample was examined by transmission electron microscope before and after ion irradiation. The results are summarized in Fig. 2.13, superimposed on the equilibrium Au-Al binary phase diagram. Diffraction measurements indicated the presence of polycrystalline Al_2Au_5 and $AlAu_2$ with a small amount of Al_2Au in the as-deposited samples over a large range of composition. After irradiation with Xe ions at a dose of 1×10^{15} ions cm^{-2}, equilibrium compounds as well as metastable alloys were observed. A solid solution was produced for the samples with a composition close to either side of the phase diagram. A metallic glass alloy was observed within the range $Al_{25}Au_{75}$ to $Al_{15}Au_{85}$. Within the remaining interval, either Al_2Au, $AlAu_2$ or a mixture of the two phases was formed depending on the film composition.

With the bilayered samples just after deposition, backscattering analysis revealed no noticeable interfacial reaction between Au and Al films. After bilayers were subjected to Xe irradiation, backscattering

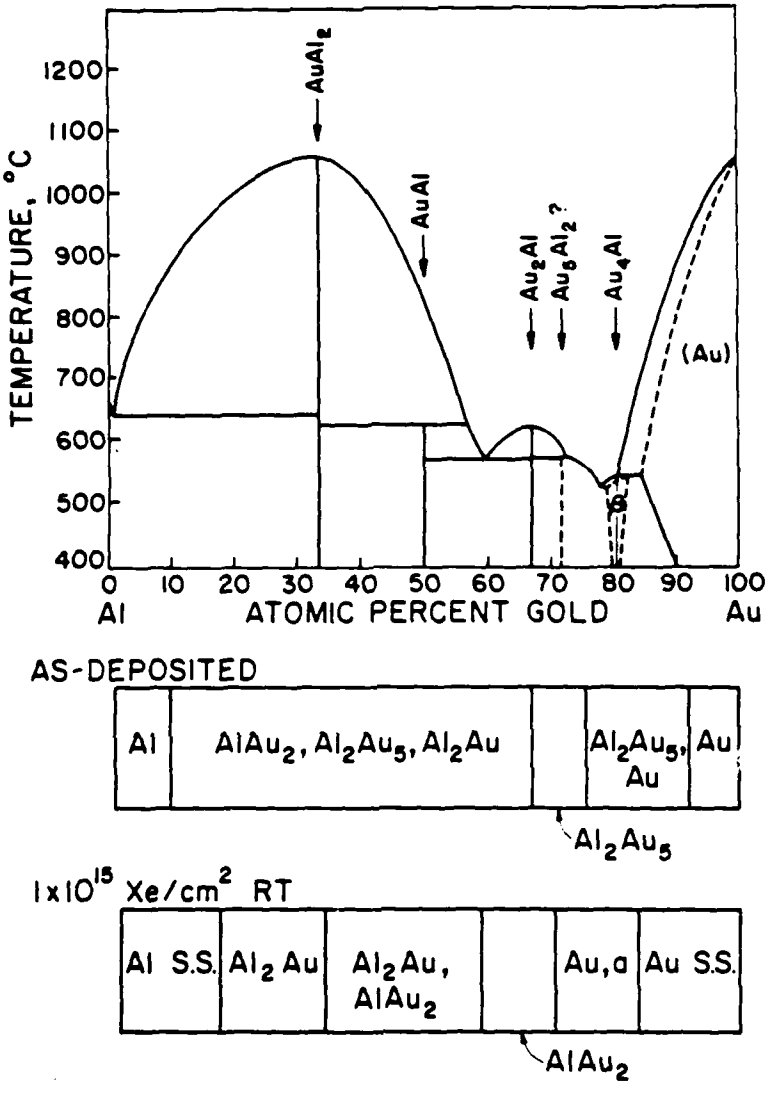

Figure 2.13. a) Equilibrium phase diagram of Au-Al, b) Composition range over which the different phases have been observed before and after ion irradiation

spectra showed a step in the Au and Al profiles, which implied the formation of a mixed layer with a composition of $AlAu_2$ (Fig. 2.14a). A prolonged irradiation resulted in the consumption of all the Au film and, later, the formation of Al_2Au at the $Al/AlAu_2$ interface (Fig. 2.14b). Ion mixing was found to be less efficient in the formation of Al_2Au than in the formation of $AlAu_2$. For instance, up to a dose of 4×10^{15} ions cm^{-2}, only one fourth of $AlAu_2$ converted into Al_2Au, whereas the dose required for the conversion of all the Au film into $AlAu_2$ is about 1×10^{15} ions cm^{-2}.

There are two major features in the present investigation, that is, the formation of complex structured compounds by ion mixing and the correlation in the phase formation between ion mixing and thermal annealing. As is stated in sections 2.2-2.4, the formation of compounds with greater complex structures than the cesium chloride structure is suppressed due to kinetic restriction. We believe that the formation of $AlAu_2$ and $AuAl_2$ by ion mixing is attributed to the appreciable atomic diffusion at room temperature. The support comes from the observation of thermal reactions in the Au-Al system where a noticeable interfacial reaction is observed at room temperatures.

It is known that initial reactions in ion mixing and thermal annealing result in identical compound formation with the systems consisted of Si and the near-noble elements (9). Such a correlation has not been found in most metal-metal systems. For instance, room temperature Xe ion irradiation of a Ni layer on Al results in the production of NiAl with the cesium chloride structure although thermal annealing shows the formation of crystalline $NiAl_3$. This observation

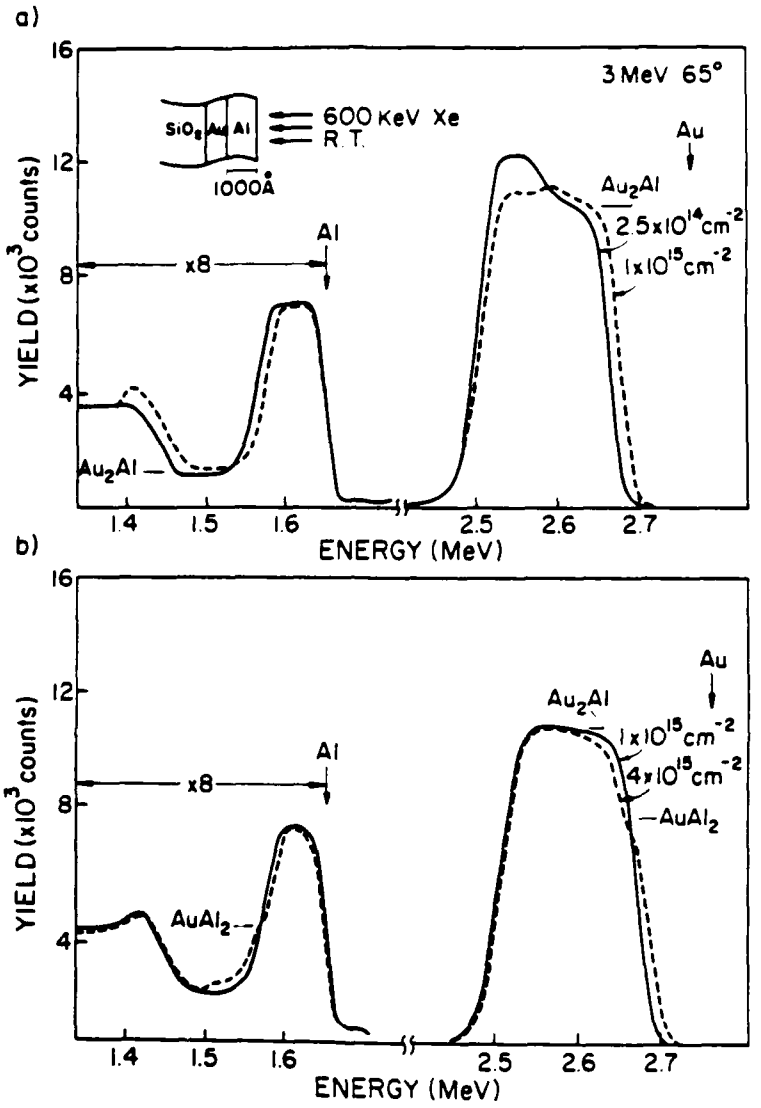

Figure 2.14. Ion backscattering spectra for SiO_2/Au/Al samples bombarded with 600 keV Xe ions to various doses, showing a) the formation of the Au_2Al compound at the Au-Al interface at low doses, and b) the formation of the $AuAl_2$ compound at the Au_2Al-Al interface at high doses.

conceivably indicates that even when the formation of a particular compound is thermodynamically favored, actual crystalline compound formation is restricted by the high quench rate in the cascade unless there is sufficient atomic mobility. In the present Au/Al case, appreciable atomic diffusion occurs at the irradiation temperature so that the implanted system acquires thermal equilibrium within implantation time. As a result of ion mixing, equilibrium compounds are formed that are correlated with compounds obtained with conventional thermal annealing.

2.6. Correlation Between the Structure of Metastable Phases and the Equilibrium Phase Diagram

In the previous sections, we show that when atomic transport is not appreciable at implantation temperatures, the formation of equilibrium compounds with complex structures is suppressed due to kinetic restrictions, leading to formation of crystalline phases with simple structures, such as solid solution and simple cubic, or amorphous alloys. When appreciable atomic diffusion occurs at target temperature, equilibrium compounds are formed that are correlated with compounds formed during conventional thermal annealing. Table 2.2 summarized the essential observation of alloy phases produced by ion mixing at room temperature reported in the literature and in the present study. Metastable alloys are formed for most of the systems investigated, whereas equilibrium compounds are only observed in a few Al-based systems. We speculate that the vacancy migration energy in Al has the lowest value of 0.62 eV among metals (33), thus thermally activated diffusion of irradiation produced defects could contribute

Table 2.2. Ion-induced phase formation in binary metal systems

Phase Observed	Binary Metal Systems
Solid Solution	Au-Ni (11,*), Au-V (11,*), Au-Co (11), Au-Fe (11) Ag-Cu (34), Ag-Ni (35), Co-Cu (1), Co-Cr (36), Au-Cu (*)
Amorphous Alloys	Mo-Ru (37), Mo-Co (37), Ti-Au (37), Ti-Ni (37) Ni-Mo (37), Ni-Nb (37), Ni-Er (37), Al-Nb (37) Al-Pt (*), Fe-W (38), Cu-Ta (39), Al-Pd (*), Al-Ni (*)
Equilibrium Compounds	Al-Pd (*), Al-Ni (*), Al-Au (*)

Remarks: (*) refers to the present work.

appreciably to the formation of equilibrium compounds at room temperature.

As is shown in Table 2.2, ion mixing is well suited for metastable phase formation. The question of our concern is how to predict the structure of metastable alloys. In the literature, a rule has been proposed to determine whether crystalline solid solutions or amorphous binary alloys are formed upon ion mixing (10, 12). The rule states that when the two components of the binary system have the same crystalline structure, but exhibit a miscibility gap in the phase diagram, supersaturated solid solutions are obtained. On the other hand, when the crystal structures of the two components are different, the tendency is to form amorphous alloys. From the present investigation, however, we found that Au and V are of different structure, but supersaturated fcc and bcc solutions are formed; Al and Pt have the same fcc structure, whereas amorphous alloys are observed over a wide range of composition. It appears that a systematic survey is necessary.

In this section, we report that the structures of metastable alloys are correlated to the commonly available phase diagram of the investigated system. Based on a comparison of the phase diagrams in the systems for which crystalline solid solutions are produced upon ion mixing, we can classify those systems into three categories: (1) simple eutectic systems, such as Ag-Cu, Au-Co, and Cu-Cr (14), (2) systems with a miscibility gap, such as Au-Fe, Au-Ni, Co-Cu, and Ag-Ni (14), and (3) systems with pronounced solubility at high temperature and several ordered compounds formed by disorder-order transition (14) (Au-Cu and Au-V) or eutectoid reaction (20) (Au-V). In the first and

second categories, the equilibrium phase diagram does not exhibit the presence of intermetallic alloys. In the third one, ordered compounds are transformed from a supersaturated solid solution and a reverse transformation occurs at high temperatures (14, 21). On the other hand, the systems for which amorphous alloys are produced by ion mixing are characterized by the presence of several intermediate phases with limited terminal solubilities between two constituents. Available experimental data indicate that the correlation is valid for all the investigated systems with Cu-Ta standing out as an exception, where an amorphous structure has been observed although Cu and Ta, similar to Ag and Ni, is an immiscible system (39).

REFERENCES

1. J. W. Mayer, B. Y. Tsaur, S. S. Lau and L. S. Hung, Nucl. Instr. and Meth. 182/183, 1 (1981).

2. J. W. Mayer and S. S. Lau, in Surface Modification and Alloying, eds. J. M. Poate, G. Foti and D. C. Jacobson (Plenum, NY, 1983), Chapter 5.

3. U. Littmark and W. O. Hofer, Nucl. Inst. and Meth., 168, 329 (1980).

4. A. Gras-Marti and P. Sigmund, Nucl. Inst. and Meth. 180, 211 (1981).

5. S. Matteson, J. Roth and M.-A. Nicolet, Radiation Effects 42, 217 (1979).

6. S. T. Picraux, D. M. Follstaedt, and J. Delafond in Metastable Materials Formation by Ion Implantation, eds., S. T. Picraux and W. J. Choyke, MRS Symposia Proc., vol. 7 (North-Holland, Amsterdam, 1982), p. 71.

7. D. H. Lee, H. R. Hart, D. A. Kiewit and O. J. Marsh, Phys. Status Solidi a 15 (1973), 645.

8. W. F. van der Weg, D. Sigurd, and J. W. Mayer, Application of Ion Beams to Metals, eds., S. T. Picraux, E. P. Ernisse, and F. L. Vook (Plenum, NY, 1974), p. 209.

9. B. Y. Tsaur, Proc. Symp. on Thin Film Interfaces and Interactions, eds. J. E. E. Baglin and J. M. Poate (The Electrochemical Society, Princeton, 1980), vol. 80-2, p. 205.

10. S. S. Lau, B. X. Liu and M.-A. Nicolet, Nucl. Instr. and Meth. 209/210, 97 (1983).

11. B. Y. Tsaur, S. S. Lau, L. S. Hung and J. W. Mayer, Nucl. Instr. and Meth. 182/183, 67 (1981).

12. B. X. Liu, W. L. Johnson, M.-A. Nicolet and S. S. Lau, Nucl. Instr. and Meth. 209/210, 229 (1983).

13. M.-A. Nicolet and S. S. Lau, in VLSI Electronics, Microstructure Science, Series edited by E. Einspruch (G. Larrabee, Guest Editor, Academic, NY, 1983), Vol. 6, Chap. 6.

14. Hansen, Constitution of Binary Alloys (McGraw-Hill, NY, 1958).

15. F. A. Shung, Constitution of Binary Alloys, Second Supplement (McGraw-Hill, NY, 1969).

16. G. Majni, C. Nobili, G. Ottaviani, Costato and E. Galli, Jour. Appl. Phys. 52, 4047 (1981).

17. S. T. Picraux and D. M. Follstaedt, in Proceedings NATO Institute on Surface Modification and Alloying (Plenun, NY, 1982), Chap. 11.

18. W. B. Pearson, Handbook of Lattice Spacings and Structure of Metals (Pergamon, NY, 1967), Vol. II, Chap. II.

19. M. W. Thompson, Defects and Radiation Damage in Metals (Cambridge University, Cambridge, England, 1969), Chap. 5.

20. W. G. Moffatt, The Handbook of Binary Phase Diagrams, G. E. Company, Schenectady, NY (1981).

21. R. Flukiger, Ch. Susz, F. Heiniger and J. Muller, Less-Common Metals 40, 103 (1975).

22. J. A. Borders and J. M. Poate, Phys. Rev. B., 13, 969 (1976).

23. J. W. Mayer, S. S. Lau, B. Y. Tsaur, J. M. Poate and J. K. Hirvonen, in Surface Modification of Materials by Ion Implantation, eds. J. K. Hirvonen and C. M. Preece (Material Researcl Soc., University Park, PA, 1979), p. 37.

24. J. Adam and R. A. Dugdale, Nature, 168, 582 (1951).

25. C. E. Dixon, C. J. Meechan and J. A. Brinkman, Phil. Mag. 44, 449 (1953).

26. R. Zee and P. Wilkes, Phil. Mag. A 42, 463 (1980).

27. C. S. Barrett and T. B. Massalski, in Structure of Metals, 3rd ed. (Pergamon, NY, 1980), Chapter 11.

28. G. Carter, D. G. Armour, S. E. Donnelly and R. Webb, Rad. Effects, 36, 1 (1978).

29. W. L. Johnson, in Proceedings of the workshop in Ion Mixing and Surface Layer Alloying, eds. S. T. Picraux and M.-A. Nicolet, 1983), p. 73.

30. J. A. Davies, in Surface Modification and Alloying, eds., J. M. Poate, G. Foti and D. C. Jacobson (Plenum, NY, 1983), Chap. 7.

31. L. E. Rehn, in Metastable Materials Formation by Ion Implantation, eds. S. T. Picraux and W. J. Choyke (Materials Research Soc., NY, 1981), p. 17.

32. E. M. Schulson, J. Nucl. Materials, 83, 239 (1979).

33. A. D. Marwick, in Surface Modification and Alloying, eds. J. M. Poate, G. Foti and D. C. Jacobson (Plenum, NY, 1983), Chap. 8.

34. B. Y. Tsaur, S. S. Lau and J. W. Mayer, Appl. Phys. Lett. 36, 823 (1980).

35. B. Y. Tsaur and J. W. Mayer, Appl. Phys. Lett. 37, 389 (1980).

36. M. Baron, J. Greggi and J. Schreurs, in Metastable Materials Formation by Ion Implantation, eds., S. T. Picraux and W. J. Choyke, Materials Research Soc. NY, 1981), p. 43.

37. B. X. Liu, W. L. Johnson, M.-A. Nicolet and S. S. Lau, Appl. Phys. Lett. 42, 45 (1983).

38. G. Goltz, R. Fernandez, M.-A. Nicolet and D. K. Sadana, in Metastable Materials Formation by Ion Implantation, eds. S. T. Picraux and W. J. Choyke, Materials Research Soc., NY, 1981), p. 227.

39. B. Y. Tsaur, Ph.D. Thesis, California Institute of Technology (1980).

40. K. N. Tu and J. W. Mayer, in Thin Films, Interdiffusion and Reactions, eds. J. M. Poate, K. N. Tu and J. W. Mayer (Wiley, NY, 1978), Chap. 10.

41. B. Y. Tsaur and C. H. Anderson, Jr., J. Appl. Phys., 53, 940 (1982).

42. H. Ishiwara, K. Hikosaka and S. Furukawa, Appl. Phys. Lett. 32, 23 (1978).

43. L. S. Wielunski, B. M. Paine, B. X. Liu, C. D. Lien and M.-A. Nicolet, Phys. Stat. Sol. (a), 72, 399 (1982).

44. D. K. Haff and Z. E. Switkowski, J. Appl. Phys. 48, 3383 (1977).

45. S. Matteson, G. Mezey and M.-A. Nicolet, in Thin Film Interface and Interactions, eds. J. E. Baglin and J. M. Poate, (Electrochemical Society, NJ, 1980), p. 242.

46. S. Matteson, B. M. Paine, M. G. Grimaldi, G. Mezey and M.-A. Nicolet, Nucl. Instr. and Meth. 182/183, 43 (1981).

APPENDIX A

James W. Mayer

Students Carrying Out Research With Backscattering Facility

Graduate Students

Larry Doolittle	August 1980 - present Thermodynamics and kinetics of thin film compound formation
Greg Galvin	August 1980 - present Transient measurements of pulsed laser annealing dynamics
Liang Sun Hung	August 1980 - present Ion beam mixing
Mike Thompson	December 1980 - present Energy coupling during pulsed laser annealing
Mike Nastasi	January 1981 - present Ion beam mixing
Long Ru Zheng	January 1981 - present Lateral silicides
Rich Fastow	June 1981 - present Pulsed ion beam annealing
Karen Kavanagh	January 1982 - present GaAs contacts
Evan Colgan	July 1982 - present Electromigration in VLSI
Edmund Zingu	August 1982 - July 1983 Silicide formation (Pd and Cr) (one year study leave from Univ. W. Cape, S. Africa)
Charles Barbour	March 1983 - present EELS study of silicides (August 1980 - March 1983 with Seidman)
Joyce Liu	September 1983 - present

Thin Film Interactions Group
Bard Hall

January 1984

Visiting Scientists and Postdoctoral Associates

Lih J. Chen	October 1980 - September 1981 National Tsing Hua University, Taiwan Electron microscopy studies of silicide formation
Chris Palmstrom	November 1980 - present Ph.D., University of LEEDS Thin film metal alloys on Si and GaAs
Giampiero Ottaviani	May 1981 - July 1981, June 1982 Institute of Physics, Univ. of Modena, Italy Silicides
Giuseppe Majni	June 1981 - August 1981 Institute of Physics, Univ. of Modena, Italy Lateral silicides
Jozsef Gyulai	October 1981 - December 1982 Central Research Institute for Physics, Budapest, Hungary Pulsed ion beam induced reactions
Rene Pretorius	October 1981 Southern Universities Nuclear Institute, South Africa Silicides
Istvan Krafcsik	July 1982 - December 1982 MEV, Budapest, Hungary Metal/metal thin film reactions
Ed Kennedy	June 1983 - August 1983 Holy Cross University Al profiling by nuclear reaction analysis
J. Olufemi Olowolafe	September 1983 - present University of Ife, Ile-Ife Nigeria Metal-Semiconductor Interactions

Rutherford Backscattering Facility Cornell Users

A. Materials Science & Engineering

1. Prof. Kramer

Prof. Kramer	-	diffusion of chlorinated hydrocarbon developer into polymer photoresists
		quantitative analysis of metal "seeds" on polymer circuit boards
Peter Green	-	marker motion in polymer-polymer diffusion
Peter Mills	-	analysis of brominated and iodated polystyrene
		quantitative determination of broken bands on a polymer fracture surface
Peter Mills & Russ Composto	-	interdiffusion in polymer blends (polystyrene-polyphenylene oxide) studied by staining with Br
Russ Composto	-	interdiffusion between polystyrene and polybromostyrene
John Romanelli	-	iodine diffusion into polyimides
Claudine Cohen	-	effect of pretreatments on etching of epoxies by chromic sulfuric acid
Claudine Cohen & Bill Vanderlinde (Prof. Ruoff)	-	diffusion of iodine into reactive ion beam etched polyimides
Phil Miller	-	evaporation of residual solvent in polymer films
Bob Bubeck (Dow Chemical)	-	iodoethanol diffusion into multilayer polymers
		diffusion of environmental stress cracking agents into polyethylene
Ron Lasky	-	Case II (non-Fickian) diffusion of iodated organics into polystyrene
Larry Berger	-	determination of chemical composition of multilayer polymer films by heavy atom staining
Steve Hudson	-	staining of electron irradiated polymers with iodine
Prof. Kramer & Peter Mills	-	Elastic recoil analysis if interdiffusion of deuterated polystyrene and hydrogenated polystyrene

2. Prof Grubb

Jay Liu	-	staining of polyethylene by chlorosulfonic acid followed by uranium acetate
Don Morel	-	RuO_4 staining of crystalline and amorphous isotactic polystyrene
		OsO_4 reactions with polystyrene surfaces
Martha Huggard	-	thickness and uniformity of spun polyimide films

3. Prof. Sass

Kurt Sickafus	-	thickness and impurity concentrations in Fe films
John Budai	-	segregation of Ag in Au bicrystals

4. Prof. Ast

Brian Cunningham	-	channeling and impurity studies of ribbon solar cell Si
Dave Lilienfeld	-	amorphous Si layer thickness
		Au diffusion in metallic glasses
Dave Lilienfeld & Tim Sullivan	-	low temperature Cu diffusion in Si
Fritz Stafford	-	defect characterization in implanted & annealed silicon-on-sapphire
Peter Zielinski	-	Composition of CuZr metallic glass ribbons

5. Prof. Johnson

Dave Kuhn	-	measurement of Pd layer thickness
Alexandra Elve	-	hydrogen profiles in metals
Lauren Heitner	-	hydrogen diffusion in Pd

6. Prof. Blakely

Dave Fowler	-	measurement of oxide thickness on Be

7. Prof. Carter

Steve Chen & Karen Kavanagh (Prof. Mayer)	-	silicides and metals on GaAs
Yonn Kouh & Ivar Reimanis	-	formation of spinels, interdiffusion of Ni and Cr oxides with sapphire

8. Prof. Ruoff

K. Balasubramanyam - Ag diffusion in inorganic resists

Tim Whetten - damage profiles in sputtered diamond

measurement of germanium selenide thickness

Bill Vanderlinde & Claudine Cohen (Prof. Kramer) - diffusion of iodine into reactive ion beam etched polyimides

B. Electrical Engineering

1. Prof. Eastman

Charles Fisher - analysis of III-V MBE layers

Collin Wood - studies of InSb-Bi compounds

Collin Stanley - analysis of GaAlInAs composition

Mark Hollis - AuGeNi contacts to GaAs

Susan Palmateer - implantation in GaAs; GaAlAs

Sayan Mukherjee - silicides on GaAs

Peter Kirchner - ohmic contacts to GaAs

2. Prof. Tang

John Kurmer - B implantation damage profiles in $LiNbO_3$ waveguides

C. National Submicron Facility

1. Ilesanmi Adesida - Ta-silicide studies

2. Prof. Wolf

Jeff Chinn - Pt, Ta, Ti, and Mo silicide studies

Ming Zhang - Ti, Mo - Silicides

D. Chemical Engineering

1. Prof. Merrill

Karel Czanderna - measurement of Al oxide thicknesses

E. Applied and Engineering Physics

1. Gerhard Schmidt - sputtered film thickness and impurity content

2. Prof. Wolga

   Natalie Gluck - evaluation of laser CVD thin films

3. Prof. Webb

   Joe Mantese - study of Ni-Al_2O_3 cosputtered films

F. Chemistry

1. Prof. Morrison

   Al Galuska - standards for SIMS analysis of GaAs-GaAlAs superlattices

   AuGeNi contacts to GaAs

   Paul Chu - calibration of SIMS samples

G. Laboratory of Plasma Studies

1. Henry Sheldon - calibration of energy analyzer for pulsed ion beam studies

H. Physics

1. Prof. Holcomb

   Paul Newman - metal contacts on silicon

2. Prof. Pohl

   Tom Klitsner - analysis of thin Au films on Si

I. Anthropology

1. Prof. Henderson & Tony Wunderlee - H profiles in obsidian for dating

   elemental analysis of archeological samples

APPENDIX D

Rutherford Backscattering Facility - Outside of Cornell Users

1. General Electric - Dave Skelly, Jim Im
   Metals on Si and SiO_2

2. Penn State University - Prof. Fonash, Arilio Clements, Rarbin Singt
   Ion beam etching of Si, Influence of ion beam etching of Si prior to metal/Si reactions

3. UC San Diego - S.S. Lau, Charles Hewitt,
   Ion beam mixing, Pulsed ion beam annealing of alloys, Metallization to GaAs

4. Northeastern University - Marwitz
   Pd on Si

5. Santa Barbara Research - Larry Lapides
   Sb-Bi on glass

6. IBM Burlington - Bruce Bertelsen, Woo Choi
   Refractory metal silicides

7. IBM Yorktown/Technion - Moshe Eizenberg
   Metallizations to Si, Thermal and pulsed ion beam annealing

8. US Army-Watertown - Forrest Burns
   Antireflection coating studies

9. Bell Labs - Barry Wilkins, Walt Augustyniack
   GaAlAs/GaAs and graphite channeling studies

10. Xerox - Joe Mort, Len Brillson, Lee Grunes, Herald Richter
    Hydrogenated silicon, Metals on III-V semiconductors (laser annealed)

11. RCA - Charles Magee
    Silicide studies, Oxide studies

12. General Ionex - Ken Purser
    Oxide and metal-metal reactions, Hydrogen in uranium

13. Kodak - Yen Tan, Wai Lam
    Diffusion studies in silver halides

14. IBM East Fishkill - Brian Cunningham
    Al/refractory metal reactions

15. Surrey University - Evan Maydell
    SiO_2/Si studies